

AFRL-ML-WP-TR-2001-4019

**UNIFIED PLASTICITY - AN ENGINEERING
APPROACH**

SOL R. BODNER

**TECHNION - ISRAEL INSTITUTE OF TECHNOLOGY
HAIFA 32000, ISRAEL**



OCTOBER 2000

FINAL REPORT FOR PERIOD 01 OCTOBER 2000 – 31 OCTOBER 2000

Approved for public release; distribution unlimited.

**MATERIALS AND MANUFACTURING DIRECTORATE
AIR FORCE RESEARCH LABORATORY
AIR FORCE MATERIEL COMMAND
WRIGHT-PATTERSON AIR FORCE BASE, OH 45433-7750**


Report Documentation Page		
Report Date 01OCT2000	Report Type N/A	Dates Covered (from... to) 01OCT2000 - 31OCT2000
Title and Subtitle Unified Plasticity-An Engineering Approach	Contract Number	
	Grant Number	
	Program Element Number	
Author(s) Bodner, Sol R.	Project Number	
	Task Number	
	Work Unit Number	
Performing Organization Name(s) and Address(es) Technion-Israel Institute of Technology Haifa 32000 Israel	Performing Organization Report Number	
Sponsoring/Monitoring Agency Name(s) and Address(es) Materials and Manufacturing Directorate Air Force Research Laboratory Air Force Materiel Command Wright-Patterson AFB, OH 45433-7750	Sponsor/Monitor's Acronym(s)	
	Sponsor/Monitor's Report Number(s)	
Distribution/Availability Statement Approved for public release, distribution unlimited		
Supplementary Notes The original document contains color images.		
Abstract		
Subject Terms		
Report Classification unclassified	Classification of this page unclassified	
Classification of Abstract unclassified	Limitation of Abstract SAR	
Number of Pages 62		

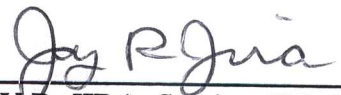
NOTICE

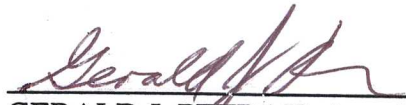
USING GOVERNMENT DRAWINGS, SPECIFICATIONS, OR OTHER DATA INCLUDED IN THIS DOCUMENT FOR ANY PURPOSE OTHER THAN GOVERNMENT PROCUREMENT DOES NOT IN ANY WAY OBLIGATE THE US GOVERNMENT. THE FACT THAT THE GOVERNMENT FORMULATED OR SUPPLIED THE DRAWINGS, SPECIFICATIONS, OR OTHER DATA DOES NOT LICENSE THE HOLDER OR ANY OTHER PERSON OR CORPORATION; OR CONVEY ANY RIGHTS OR PERMISSION TO MANUFACTURE, USE, OR SELL ANY PATENTED INVENTION THAT MAY RELATE TO THEM.

THIS REPORT IS RELEASABLE TO THE NATIONAL TECHNICAL INFORMATION SERVICE (NTIS). AT NTIS, IT WILL BE AVAILABLE TO THE GENERAL PUBLIC, INCLUDING FOREIGN NATIONS.

THIS TECHNICAL REPORT HAS BEEN REVIEWED AND IS APPROVED FOR PUBLICATION.


THEODORE NICHOLAS
Metals Branch
Metals, Ceramics & NDE Division


JAY R. JIRA, Section Chief
Behavior & Life Prediction
Metals, Ceramics & NDE Division


GERALD J. PETRAK, Asst Chief
Metals, Ceramics & NDE Division
Materials and Manufacturing Directorate

Disclaimer

Any opinions, findings and conclusions or recommendations expressed in this material are those of the author and do not necessarily reflect the views of the European Office of Aerospace Research and Development, Air Force Office of Scientific Research, Air Force Research Laboratory.

Do not return copies of this report unless contractual obligations or notice on a specific document requires its return.

REPORT DOCUMENTATION PAGE					Form Approved OMB No. 0704-0188	
The public reporting burden for this collection of information is estimated to average 1 hour per response, including the time for reviewing instructions, searching existing data sources, gathering and maintaining the data needed, and completing and reviewing the collection of information. Send comments regarding this burden estimate or any other aspect of this collection of information, including suggestions for reducing the burden, to Department of Defense, Washington Headquarters Services, Directorate for Information Operations and Reports (0704-0188), 1215 Jefferson Davis Highway, Suite 1204, Arlington, VA 22202-4302. Respondents should be aware that notwithstanding any other provision of law, no person shall be subject to any penalty for failing to comply with a collection of information if it does not display a currently valid OMB control number.						
PLEASE DO NOT RETURN YOUR FORM TO THE ABOVE ADDRESS.						
1. REPORT DATE (DD-MM-YYYY) October 2000		2. REPORT TYPE Final Report			3. DATES COVERED (From - To) 10/01/2000 - 10/31/2000	
4. TITLE AND SUBTITLE Unified Plasticity - An Engineering Approach				5a. CONTRACT NUMBER N/A		
				5b. GRANT NUMBER N/A		
				5c. PROGRAM ELEMENT NUMBER 61102F		
				5d. PROJECT NUMBER 2302		
6. AUTHOR(S) Sol R. Bodner				5e. TASK NUMBER ED		
				5f. WORK UNIT NUMBER L4		
7. PERFORMING ORGANIZATION NAME(S) AND ADDRESS(ES) Technion - Israel Institute of Technology Haifa 32000 Israel				8. PERFORMING ORGANIZATION REPORT NUMBER		
9. SPONSORING/MONITORING AGENCY NAME(S) AND ADDRESS(ES) MATERIALS AND MANUFACTURING DIRECTORATE AIR FORCE RESEARCH LABORATORY AIR FORCE MATERIEL COMMAND WRIGHT-PATTERSON AIR FORCE BASE, OH 45433-7750				10. SPONSOR/MONITOR'S ACRONYM(S) <u>AFRL/MLLMN</u>		
				11. SPONSOR/MONITOR'S REPORT NUMBER(S) AFRL-ML-WP-TR-2001-4019		
12. DISTRIBUTION/AVAILABILITY STATEMENT Approved for public release; distribution is unlimited.						
13. SUPPLEMENTARY NOTES <u>CONTAINS SOFTWARE CODE.</u>						
14. ABSTRACT A review of the elastic-viscoplastic constitutive theory of Bodner-Partom is presented with emphasis on the physical motivations. The governing equations, which do not include a yield criterion or loading/unloading conditions, are intended to represent the mechanical behavior of metals over a wide range of strain rates and temperatures and for general loading circumstances. Those equations include load-history-dependent state variables to indicate isotropic and directional hardening and could also incorporate continuum damage as a softening variable. Possible modifications of the basis equations may be necessary to describe particular material effects. A method is suggested for identification of the material parameters from test data, and parameter values for a number of metals obtained by various investigators are tabulated. A procedure for numerical integration of the constitutive equations is outlined and used to obtain simulations for exercises involving monotonic and cyclic loadings. Also included is an extensive list of references, some of which describe the incorporation of the constitutive theory into finite element and finite difference numerical programs.						
15. SUBJECT TERMS Unified Constitutive Equations, Viscoplasticity						
16. SECURITY CLASSIFICATION OF:			17. LIMITATION OF ABSTRACT		18. NUMBER OF PAGES	
a. REPORT UL	b. ABSTRACT UL	c. THIS PAGE UL	SAR		96	
					19a. NAME OF RESPONSIBLE PERSON Theodore Nicholas <u>AFRL/MLLMN</u>	
					19b. TELEPHONE NUMBER (Include area code) 937-255-1347	

Contents

List of Figures	iv
Preface	vi
Acknowledgements	vi
1. Introduction	1
2. Concepts and Basic Equations	2
3. Extensions and Applications of the Basic Equations	13
3.1 Variable rate of hardening/cyclic loading	13
3.2 Strain rate dependence of hardening rate	14
3.3 Creep of metals	15
3.4 Continuum damage as a state variable	17
3.5 Non-proportional loadings	20
3.6 Viscoplastic buckling	20
4. Integration of Constitutive Equations	25
5. Material Constants and Applications	28
5.1 Background	28
5.2 Methods for determination of material constants	29
5.3 Examples	32
6. Further Developments	49
7. Summary - Status of the B-P Constitutive Theory	51
References	52
Appendix A - Computer Program	62
Appendix B - Nomenclature	66
Figures	70

List of Figures

Figure	Page
1: Inelastic strain rates for uniaxial tension, σ_{11} , and various values of n	71
2: Dependence of the uniaxial flow stress parameter on the strain rate parameter for various values of the strain rate sensitivity constant n	71
3: Dependence of the uniaxial flow stress parameter on the (temperature dependent) strain rate sensitivity constant n for different values of the strain rate parameter	72
4: Simulation by Bodner and Lindenfeld (1995)	73
5: Flow stress dependence of copper on logarithm of strain rate	74
6: Representation of identical stress-strain curves for different combinations of n and Z_0 with m_1 and Z_1/Z_0 fixed	75
7: Effect of rate-sensitivity parameter n on stress relaxation behavior with the same material constants used in Fig. 6	75
8: Effect of rate sensitivity parameter n on stress-strain behavior at various imposed rates with the same material constants used in Figs. 6,7	76
9: Loading, unloading, and re-loading stress-strain curves for $n = 1$ and associated constants; initial loading $\dot{\epsilon} = 10^3 \text{ sec}^{-1}$	77
10: Effect of changes of imposed strain rate on stress-strain response for $n = 1$ and associated constants	78
11: Stress-strain curves upon loading, unloading and reversed loading for isotropic hardening (I) only, and with isotropic (I) and directional hardening (D), for $n = 1$ and associated constants with $m_2 = m_1$, $\dot{\epsilon} = 10^{-3} \text{ sec}^{-1}$	79
12a: Cyclic stress-curves, $n = 1$ and associated constants, $m_2 = m_1$, $\dot{\epsilon} = 10^{-3} \text{ sec}^{-1}$, isotropic hardening only	80
12b: Cyclic stress-curves, $n = 1$ and associated constants, $m_2 = m_1$, $\dot{\epsilon} = 10^{-3} \text{ sec}^{-1}$, combined isotropic and directional hardening	81
13: Stress-strain curves for $n = 1$ and associated constants, $\dot{\epsilon} = 10^3 \text{ sec}^{-1}$	82

14:	The isotropic and directional hardening components of B1900+Hf in an η - σ plot [from Chan et al	83
15:	Comparison of the experimental data of Gray et al. (1994) for compression with the Bodner-Partom model simulations taking $Z_1 \rightarrow Z_1(T)$	83
16:	Plots of stresses and associated steady strain rates	84

Author's Preface

Unified theories of elastic-viscoplastic material behavior, which are primarily applicable for metals and metallic alloys, combine all aspects of inelastic response into a set of time dependent equations with a single inelastic strain rate variable. Those equations may or may not include a yield criterion, but models which do not separate a fully elastic region from the overall response could be considered "unified" in a more general sense. The theories have reached a level of development and maturity where they are being used in a number of sophisticated engineering applications. However, they have not yet become a standard method of material representation for general engineering practice.

This report describes the background and capability of a particular formulation by Bodner and Partom (B-P) to enable it to be more accessible to the engineering community. Publications on the topic have appeared in journals and in conference proceedings over the past 30 years and part of the purpose of this report is to consolidate the information. Results of a number of exercises by various authors on the further development and application of the B-P theory are also described. The listings and discussions of those investigations are intended to be representative and not comprehensive. With these objectives, it is hoped that the report will serve as a useful reference for modelling the mechanical behavior of materials over a wide range of circumstances.

Sol R. Bodner
e-mail: mersbod@techunix.technion.ac.il

Disclaimer

Any opinions, findings and conclusions or recommendations expressed in this material are those of the author and do not necessarily reflect the views of the European Office of Aerospace Research and Development, Air Force Office of Scientific Research, Air Force Research Laboratory.

Acknowledgements

The author wishes to thank his colleague, Prof. Miles B. Rubin, for the extensive discussions we had on this article and for providing the program for numerical integration of the constitutive equations with the resulting simulations.

He also wishes to thank Mrs. Bernice Hirsch of the Technion for her excellent preparation of the report.

Most of the research work on the development of the constitutive equations described in this article was supported by grants from the US Air Force of Scientific Research through the European Office of Aerospace Research and Development (EOARD), US Air Force.

This report is based upon work supported by the European Office of Aerospace Research and Development, Air Force Office of Scientific Research, Air Force Research Laboratory, under Contract No. F61775-00-WE024. Declarations

The Contractor, Technion - Israel Institute of Technology, hereby declares that, to the best of its knowledge and belief, the technical data delivered herewith under Contract No. F61775-00-WE024 is complete, accurate, and complies with all requirements of the contract.

25 October 2000

Prof. Sol R. Bodner
Dept. of Mechanical Engineering
Technion - Israel Institute of Technology
Haifa 32000, Israel.

I certify that there were no subject inventions to declare as defined in FAR 52.227-13, during the performance of this contract.

25 October 2000

Prof. Sol R. Bodner
Dept. of Mechanical Engineering
Technion - Israel Institute of Technology
Haifa 32000, Israel.

UNIFIED PLASTICITY - AN ENGINEERING APPROACH

1. Introduction

The mechanical behavior of materials is an essential component of Technology which has received considerable attention over many years. Of particular interest is the response of materials to mechanical and thermal loadings, the influence of environmental factors, and the conditions and mechanisms of failure. The terms "constitutive equations" and "material modelling" are usually applied to the analytical representation of the material response characteristics prior to total failure. There have been considerable advances on this subject in recent years due to better understanding of the physics of deformation and the advent of efficient computational capability which enables solution of complicated equations.

This article is concerned with a particular approach for representing the time dependent inelastic behavior of isotropic polycrystalline solids as part of a combined elastic-inelastic formulation that does not rely on a yield criterion or loading and unloading conditions. The same equations are intended to apply for all loading circumstances such as straining at prescribed rates, creep under constant stress, and stress relaxation under constant strain; hence the term "unified" has been suggested for this class of constitutive equations. An objective of a unified constitutive theory is that it be applicable for certain classes of materials over a wide range of strain rates and temperatures. To be useful for engineers, the equations should be reasonably simple and have a firm physical basis and be consistent with the principles and constraints of Mechanics and Thermodynamics. It is noted that much of the work of materials scientists is motivated and intended for the development and improvement of materials and does not particularly address the needs of structural and mechanical engineers. As a consequence, care has to be exercised in transferring information and terminology from one field to the other. Also, the formulation should consider associated matters such as the determination of material parameters from test data and the implementation of the equations in computer programs.

The direction taken for the development of the unified constitutive equations described here, those of Bodner and Partom (B-P), was that the overall framework should be consistent with the essential physics of elastic and inelastic deformations. In contrast to classical plasticity theory, those equations do not require a yield criterion or loading and unloading conditions. Details are intended to represent the principal macroscopic response properties such as strain rate sensitivity and temperature dependence of inelastic deformation, stress saturation under imposed straining, isotropic and directional hardening for both monotonic and reversed loadings, primary and secondary creep, thermal recovery of hardening, and stress relaxation. Since attention was given to the underlying physics in the development of the equations, recourse to specific microscopic mechanisms was not necessary.

Publications on the reference unified constitutive equations have appeared since that of Bodner (1968) and have been spread over many journals and conference proceedings. The present article is intended to consolidate the information and also to serve as a general introduction to the subject. A review paper was published by Bodner (1987), but there have

been a number of contributions since then. In fact, the subject is approaching a level of maturity where it could be considered as a standard method for representing material response behavior. Other sets of unified constitutive equations have been proposed and some of them are referred to in this article. However, it is not the intention here to provide descriptions of all unified plasticity models or to make comparisons or offer criticisms. It is left to the practitioners of the art of engineering to decide what is useful for their purposes.

2. Concepts and Basic Equations

Most of the discussion in this article is concerned with the small strain case where the elastic (fully reversible) and inelastic (non-reversible) strain rates are simply additive. A primary supposition in a formulation without a yield criterion is that both elastic and inelastic strain rates are generally non-zero at all stages of loading and unloading. For sufficiently accurate measurements, most all materials behave in that manner as described in Bell's (1973) historical review of the works of Hodgkinson - 1843, Wertheim - 1844, Bauschinger - 1886, von Kármán - 1911, and others. However, it was the success of the theoretical elasticians and subsequently the needs of engineering over more than 100 years that enshrined the concept of a pure elastic range bounded by a yield criterion. Regarding "post-yield" hardening, R. Hill, who has made significant contributions to classical plasticity and authored an early important book on plasticity theory, Hill (1950), has recently questioned the usefulness of a distinct global yield function as a reference for hardening, Hill (1994).

The unified plasticity approach is based on the use of a single variable to represent all inelastic deformations and could be developed in formulations with or without a yield criterion. In the former case, it would be applied only in the non-fully elastic range. To illustrate the approach in the absence of a yield condition, such as the B-P theory, it is useful to consider the case of uniaxial stress, σ_{11} , in a uniform rod of homogeneous isotropic material at a constant temperature. For assumed small strains,

$$\dot{\epsilon}_{11} = \dot{\epsilon}_{11}^e + \dot{\epsilon}_{11}^p \quad (1)$$

where $\dot{\epsilon}_{11}$ is the axial deformation velocity gradient or, in the case of assumed small strains, the total axial strain rate, and both strain rate components are generally non-zero. The elastic axial strain rate $\dot{\epsilon}_{11}^e$ is obtainable from an elastic stress-strain relation, e.g. $\dot{\epsilon}_{11}^e = \dot{\sigma}_{11}/E$, where E is Young's modulus. Based on physical grounds and consistency with mechanical principles, the axial inelastic (plastic) strain rate $\dot{\epsilon}_{11}^p$ can be assumed to be a function of current values of state quantities and particularly of stress σ_{11} , load history dependent internal state variables Z_g , total axial strain rate $\dot{\epsilon}_{11}$, and temperature T , i.e.,

$$\dot{\epsilon}_{11}^p = f(\sigma_{11}, Z_g, \dot{\epsilon}_{11}, T) \quad (2)$$

In most applications of the unified approach, the possible dependence of $\dot{\epsilon}_{ij}^p$ on $\dot{\epsilon}_{ij}$ is ignored.

Under conditions of imposed constant total axial strain rate $\dot{\epsilon}_{11} = R_1$ and constant temperature as in a standard uniaxial tensile test, eq. (1) could be integrated in time to provide a stress-strain curve at the prescribed rate. A stress-strain curve, therefore, is not a basic material property but the consequence of a particular test arrangement and test conditions while the material properties are given by the expressions for $\dot{\epsilon}_{11}^e$ and $\dot{\epsilon}_{11}^p$. [Of

course, a standard stress-strain curve at a low strain rate is useful as a measure of material strength in many engineering applications.] For the stressed uniform rod, unloading at a given stress and strain condition could be achieved by reversing the imposed strain rate, say to $-R_1$. Eq. (1) would still apply with $\dot{\epsilon}_{11} = -R_1$ which can again be integrated in time. With a theory without a yield criterion, both elastic and inelastic strains would be realized during the complete unloading process to zero stress although the contribution of $\dot{\epsilon}_{11}^P$ would be very small at low stress levels. That is, unlike classical elastic-plastic theory, unloading is not fully elastic. A yield criterion would require that $\dot{\epsilon}_{11}^P = 0$ for stress levels in the fully elastic range. For creep conditions at constant temperature, the axial stress σ_{11} is constant so that $\dot{\epsilon}_{11}^e$ is zero and $\dot{\epsilon}_{11} = \dot{\epsilon}_{11}^P$, eq. (2), which provides the relation for the change of axial strain with time. In the case of constant total axial strain imposed subsequent to a straining history, $\dot{\epsilon}_{11} = 0$ so that $\dot{\epsilon}_{11}^e = \dot{\sigma}_{11} / E = -\dot{\epsilon}_{11}^P$ and stress relaxation takes place. With the unified formulation, plasticity, creep, and stress relaxation are consequences of particular loading conditions and are not separate material properties.

Applying the unified representation to actual materials, particularly metals, involves generalizing the equation for $\dot{\epsilon}_{11}^P$ to the multi-dimensional case and using specific analytical expressions. Also, since plastic deformation is considered to be incompressible and thermal expansion is dilatational, it may be more convenient in some applications to separate the isotropic stress-strain relations into deviatoric and dilatational components,

$$s_{ij} = 2G(e_{ij} - e_{ij}^P), \quad i, j, k = 1, 2, 3 \quad (3a)$$

$$\sigma_{kk} = 3K[\epsilon_{kk} - 3\alpha(T - T_0)] \quad ()_{kk} \Rightarrow \sum_{k=1}^3 ()_{kk} \quad (3b)$$

where G is the shear modulus, K is the bulk modulus, T_0 is the reference temperature, and α is the thermal expansion coefficient which should be appropriately defined in the temperature range from T_0 to T . The deviatoric stress and strain rates are defined by:

$s_{ij} = \sigma_{ij} - (1/3)\sigma_{kk}\delta_{ij}$ and $\dot{e}_{ij} = \dot{\epsilon}_{ij} - (1/3)\dot{\epsilon}_{kk}\delta_{ij}$ where δ_{ij} is the Kronecker delta function ($\delta_{ij} = 1, i = j$; $\delta_{ij} = 0, i \neq j$). Due to incompressibility of plastic deformation, $\dot{\epsilon}_{kk}^P = 0$, the plastic strain rate is deviatoric, $\dot{\epsilon}_{ij}^P = \dot{e}_{ij}^P$. Under non-isothermal loadings, the elastic moduli G and K , which are simply related to the usual engineering moduli E and ν , and the thermal expansion coefficient α are generally functions of temperature T . To obtain the differential form of eqs. (3a), (3b) accounting for temperature changes in the material constants, the full time derivative of those equations is evaluated,

$$\dot{s}_{ij} = 2G(\dot{e}_{ij} - \dot{e}_{ij}^P) + 2(e_{ij} - e_{ij}^P)\frac{\partial G}{\partial T}\dot{T} \quad (3c)$$

$$\begin{aligned} \dot{\sigma}_{kk} = & 3K(\dot{\epsilon}_{kk} - 3\alpha\dot{T}) \\ & + 3[\epsilon_{kk} - 3\alpha(T - T_0)]\frac{\partial K}{\partial T}\dot{T} - 9K(T - T_0)\frac{\partial \alpha}{\partial T}\dot{T} \end{aligned} \quad (3d)$$

where G , K and α and their temperature derivatives are the current values at T .

As in eq. (2), the multi-dimensional plastic strain rate $\dot{\epsilon}_{ij}^P$ is a function of current values of state quantities,

$$\dot{\epsilon}_{ij}^P = \dot{\epsilon}_{ij}^P = f(\sigma_{ij}, Z_g, \dot{\epsilon}_{ij}, T) \quad (4)$$

where the load history dependent variables Z_g are considered to represent the hardened state of the material with respect to resistance to plastic flow, and $\dot{\epsilon}_{ij}$ is the total strain rate. The influence of temperature on $\dot{\epsilon}_{ij}^P$ is discussed later and temperature history effects due to non-isothermal conditions can usually be described using data obtained from isothermal tests. Certain microscopic processes, however, such as dynamic strain ageing could lead to inverse strain rate and temperature history effects over some range of strain rates and temperatures and require particular analyses which are not considered here.

The proposed expression for $\dot{\epsilon}_{ij}^P$ is based on the isotropic form of the Prandtl-Reuss flow law which is taken to be a physical law by itself independent of a yield criterion,

$$\dot{\epsilon}_{ij}^P = \dot{\epsilon}_{ij}^P = \lambda s_{ij} \quad ; \quad \dot{\epsilon}_{kk}^P = 0 \quad : \quad \lambda \geq 0 \quad (5)$$

where λ is a scalar function of current state quantities. Equation (5) states that plastic straining is in the direction of deviatoric stress and that plastic deformation is incompressible. Squaring eq. (5) leads to

$$D_2^P = \lambda^2 J_2 \quad , \quad \lambda = (D_2^P / J_2)^{1/2} \quad (6)$$

where $D_2^P = (1/2) \dot{\epsilon}_{ij}^P \dot{\epsilon}_{ij}^P$ and $J_2 = (1/2) s_{ij} s_{ij}$ are the second scalar invariants of deviatoric plastic strain rate and deviatoric stress respectively and are coordinate-independent.

Proposing an expression for D_2^P in the form of equation (4) would then enable λ in equations (5,6) to be determined. Engineers usually find it more convenient to work with the effective values of plastic strain rate,

$$\dot{\epsilon}_{\text{eff}}^P = \dot{\epsilon}_{\text{eff}}^P = (2/\sqrt{3}) (D_2^P)^{1/2} = \left(\frac{2}{3} \dot{\epsilon}_{ij}^P \dot{\epsilon}_{ij}^P \right)^{1/2} \quad (6a)$$

and effective stress

$$\sigma_{\text{eff}} = (3J_2)^{1/2} = \left(\frac{3}{2} s_{ij} s_{ij} \right)^{1/2} \quad (6b)$$

which can be expressed in terms of the respective components and reduced in the uniaxial stress case to $\dot{\epsilon}_{11}^P$ and σ_{11} .

A number of expressions for $\dot{\epsilon}_{11}^P$ appear in the materials science literature that are intended to correspond to particular thermally activated dislocation mechanisms. Rather than use any of these functions, a general growth law is employed which has the desirable properties that plastic strain rate is very small at low stresses and has a limiting saturation value at high stresses. The proposed expression relating the invariants of plastic strain rate and stress is as follows:

$$D_2^P = D_0^2 \exp \left[- \left(\frac{Z^2}{\sigma_{\text{eff}}^2} \right)^n \right] \quad (7)$$

This form has been used in the social and biological sciences and, as shown in Fig. 1, has ranges of incubation, rapid growth, and saturation. In eq. (7), n controls the rate of growth and thereby rate sensitivity, Z is interpreted as the load history dependent scalar "hardening" parameter, i.e. an internal state variable, which could have isotropic and directional components, and D_0 is the limiting value of D_2^P at high stress and acts as a scale factor in the equation. From an overall physical viewpoint, n controls the inherent "viscosity" of inelastic flow and Z is a measure of resistance to inelastic deformation which is directly related to the micro-structural arrangements responsible for the so-called stored energy of cold work (SECW). Both n and Z are generally and separately temperature dependent so that an explicit temperature term does not appear in eq. (7) which can be considered to be a general macroscopic description of inelastic response due to "thermally activated" dislocation mechanisms. Although the plastic flow law, eq. (5), indicates no plastic volume change, dependence on pressure could be included parametrically through n and/or Z .

Substituting eq. (7) into eqs. (6) and (5) leads to a general expression for the plastic strain rate components,

$$\dot{\epsilon}_{ij}^P = D_0 \exp \left[- \frac{1}{2} \left(\frac{Z^2}{\sigma_{\text{eff}}^2} \right)^n \right] \frac{\sqrt{3} s_{ij}}{\sigma_{\text{eff}}} \quad (8)$$

and the particular cases of uniaxial stress σ_{11} and simple shear τ_{12} are,

$$\dot{\epsilon}_{11}^P = \frac{2}{\sqrt{3}} \left(\frac{\sigma_{11}}{|\sigma_{11}|} \right) D_0 \exp \left[- \frac{1}{2} \left(\frac{Z}{\sigma_{11}} \right)^{2n} \right] \quad (9)$$

$$\dot{\epsilon}_{12}^P = \frac{1}{2} \dot{\gamma}_{12}^P = D_0 \left(\frac{\tau_{12}}{|\tau_{12}|} \right) \exp \left[- \frac{1}{2} \left(\frac{Z}{\sqrt{3}\tau_{12}} \right)^{2n} \right] \quad (10)$$

where $\dot{\gamma}_{12}$ and τ_{12} are the engineering shear strain rate and stress.

Linear and semi-logarithmic plots of eq. (9) in non-dimensional coordinates are shown in Figs. 1 and 2, but the curves in Fig. 1 are not physically meaningful beyond $\sigma_{11}/Z = 1$ except to show the limiting inelastic strain rate. It is seen that the parameter n controls rate sensitivity and as n becomes large for a given plastic strain rate, the non-dimensional stress term σ_{11}/Z approaches unity and its rate dependence diminishes. Rate independent plasticity is therefore a limiting case in the formulation. The parameter n also has an influence on the stress level in addition to that of the hardening variable Z . It would be expected that n should normally vary inversely with temperature. Increasing temperature would therefore lower n leading to enhanced rate sensitivity and a reduced level of the stress-strain curves, e.g. Fig. 3 which is a plot of eq. (9) for assumed $(T/a) = 1/n$ (where "a" is a material constant). An empirical form that serves as a reasonable approximation for some metals is $n = A + (B/T)$. Inversely, as the temperature approaches absolute zero, n would

become large leading to $\sigma_{11} = Z$ which is referred to as the rate independent "mechanical threshold stress" for thermally activated deformation mechanisms.

According to eq. (8), an increase in Z corresponding to increased resistance of plastic flow would require a stress increase to maintain the same plastic strain rate. Usual measures of the hardened state are plastic work and accumulated plastic strain. Plastic work is generally preferred by investigators in Solid Mechanics, e.g. Hill, (1950), and leads to better agreement with strain rate jump tests. With plastic work rate (per unit volume) $\dot{W}_p = \sigma_{ij} \dot{\epsilon}_{ij}^p = \sigma_{eff} \dot{\epsilon}_{eff}^p$ as the hardening rate measure, a suitable and simple evolution equation for isotropic hardening Z^I is,

$$\dot{Z}^I(t) = m_1[Z_1 - Z^I(t)]\dot{W}_p(t) - A_1 Z_1 \left[\frac{Z^I(t) - Z_2}{Z_1} \right]^{r_1} \quad (11)$$

with the initial condition $Z^I(0) = Z_0$. In the first term, Z_1 is the limiting (saturation) value of Z^I and m_1 controls the hardening rate. The negative part of the first term is necessary to ensure that stress-strain curves saturate; otherwise the response would revert to elastic behavior at large W_p . It is referred to as "dynamic recovery" in the materials science literature.

The second term of eq. (11) corresponds to thermal recovery of hardening with Z_2 as the minimum value at a given temperature and A_1, r_1 are temperature dependent material constants. Straining from the fully annealed (recovered) condition would generally require $Z_0 = Z_2$. Consideration of thermal recovery of hardening is essential for high temperature applications and secondary (constant rate) creep is the condition under constant stress at which $\dot{Z}^I = 0$ or Z becomes constant. Secondary creep could also occur in the absence of thermal recovery of hardening by the hardening values reaching saturation; in the case of only isotropic hardening, when $Z^I = Z_1$. A more extensive discussion of creep of metals appears in a subsequent section.

As noted previously, probable temperature dependence of the overall hardening variable Z in the general response equation (8) has to be considered. A possible method could be based on multiplying Z by a continuous function of T which is determined empirically as in the Johnson-Cook equation, e.g. $(1 - T^{*d})$, where $T^* = (T - T_0)/(T_m - T_0)$ and T_m is melting, T_0 is reference ($T \geq T_0$), and d is an empirical value. Alternatively, the minimum and maximum values of the hardening parameters Z_0 and Z_1 could be considered to be functions of temperature according to the empirical expression. However, that function would approach zero at melting which would lead to unrealistic values of plastic strain rate so its applicability is limited.

An exercise for representing stress-strain test results for annealed pure copper by the B-P equations over a range of temperature, RT to 800°C, and at a constant strain rate of 2000/sec was carried out by Bodner and Rajendran (1996). Isotropic hardening with the saturation value Z_1 reducing bi-linearly with temperature led to very good agreement with the test stress-strain curves over the above temperature range, Fig. 15. Since the test data was available only at a single applied strain rate, it was not possible in this exercise to determine the effect of temperature on the parameter n which controls rate sensitivity as well as

influences the level of stress-strain curves. Hardening has a major role on the response of annealed copper and the ratio Z_1/Z_0 is relatively large, 12.8. Strain rate appears to have a strong effect on the hardening rate of copper at very high strain rates, which is discussed in a subsequent section.

Generally, it has been found that values of the material constants obtained from isothermal tests at various temperatures can be used in non-isothermal applications with satisfactory results, Chan and Lindholm (1990b). Unusual temperature history effects due to very specific metallurgical mechanisms, such as dynamic strain ageing, are excluded and require separate treatment. From the computational viewpoint, this means that listings or analytical approximations of the material constants as functions of temperature should be part of the numerical procedure for non-isothermal conditions. An alternative, more formal method was suggested by Moreno and Jordan (1986), based on expanding the evolution

equation for isotropic hardening, eq. (11), to include terms dependent on temperature rate \dot{T} . As an example, an expression for \dot{Z}^I , in which thermal recovery of hardening is neglected, can be taken to be the basic representation for isotropic hardening rather than the evolution equation (11), i.e.

$$Z^I = Z_1 - (Z_1 - Z_0) \exp(-m_1 W_p) \quad (12)$$

where W_p is the accumulated plastic work (per unit volume) commencing from zero for $Z^I = Z_0$. Considering the parameters m_1 , Z_0 , Z_1 to be temperature dependent leads to,

$$\begin{aligned} \dot{Z}^I = m_1 [Z_1 - Z^I] \dot{W}_p \\ + \left[\frac{dZ_1}{dT} + W_p (Z_1 - Z^I) \frac{dm_1}{dT} - \left(\frac{Z_1 - Z^I}{Z_1 - Z_0} \right) \left(\frac{dZ_1}{dT} - \frac{dZ_0}{dT} \right) \right] \dot{T} \end{aligned} \quad (13)$$

Equation (13) indicates that increasing temperature in the primarily elastic range for which $W_p \sim 0$, $\dot{W}_p \sim 0$ and $Z^I \sim Z_0$ results in $\dot{Z}^I = \frac{dZ_0}{dT} \dot{T}$ which would be non-zero and negative valued. As a consequence, the stress level for the onset of significant inelastic straining, which is dependent on Z_0 , is reduced. The same result would be obtained using the original hardening evolution equation (11) and an appropriate numerical procedure that includes the dependence of Z_0 , and also Z_1 and m_1 , on temperature.

In eq. (10), D_0 represents the limiting plastic strain rate in shear as the shear stress becomes large or as the hardening parameter Z approaches zero. An interesting question is whether such a limit exists physically. Referring to Orowan's equation for the plastic strain rate as a function of mobile dislocation velocity and density, suitable maximum values lead to a shear strain rate of the order of $10^8/\text{sec}$ with material dependent variations. Also, numerical exercises are now in progress which attempt to simulate atomic arrays with dislocation like defects subjected to extreme loadings and temperatures, e.g. Holian and Lomdahl (1998). Preliminary results indicate that a limiting plastic strain rate appears to exist as long as the arrays act as a crystalline solid but the response transits to viscous fluid-like behavior at very high stresses or at melting. A modification of the constitutive theory to represent this behavior has been proposed by Rubin (1987). From the viewpoint of application of the constitutive equations to engineering problems, this discussion implies that D_0 is a meaningful physical quantity that would be material dependent over a limited range. It is appreciably above the strain rates in most applications, and should be specified in advance i.e. it should have an assigned value, and not be part of the determination of material constants from conventional test data. The same conclusion was reached by Mahnken and Stein (1996) based on studies of the numerical stability of the process for material parameter determination.

In the initial applications of unified constitutive equations, most of the practical interest was on problems of high temperature creep and related topics in the quasi-static range with strain rates generally less than 1 sec^{-1} . For this reason and to avoid numerical difficulties with the available computational techniques, it seemed adequate to set the parameter D_0 in the basic kinetic equations (7), (8), to be 10^4 sec^{-1} . A number of sets of material constants were determined on that basis with good agreement between the numerical simulations and test results. More recently, unified constitutive models are used in problems involving high strain

rates such as dynamic loadings and shock wave propagation so the more physically based value of $D_0 = 10^8 \text{ sec}^{-1}$ is utilized in the equations. In a subsequent section, sets of material constants are described for various metals based on either of the two values of D_0 . It is suggested that the sets of constants using the lower value of D_0 be limited to applications with strain rates less than 10 sec^{-1} . With the presently available numerical schemes for integrating the equations, as described in a subsequent section, there is no difficulty in using $D_0 = 10^8 \text{ sec}^{-1}$ and associated constants for the lowest strain rates. It is noted that the values of the materials constants depend upon the choice of D_0 .

Many practical applications can be served using eq. (8) and isotropic hardening, eq. (11), and some are described in a later section. For interest, those equations were first published in a conference proceedings, Bodner and Partom (1972a), and in a reference journal, Bodner and Partom (1975). Numerical solution of the equations is generally necessary and suitable procedures have been developed. In the particular case of uniaxial stress σ_{11} and constant plastic strain rate, $\dot{\epsilon}_{11}^P = R$, and the absence of thermal recovery of hardening, the equations can be readily integrated, Merzer and Bodner (1979), leading to an analytical expression for the stress-strain relation,

$$\left[(\sigma_s - \sigma_{11}) / \sigma_{11} \right] = \sigma_s C_1 \exp \left\{ -m_1 \sigma_s \left[\epsilon_{11} - (\sigma_{11}/E) \right] \right\}. \quad (14)$$

Here, $\sigma_s = K_1 Z_1$ is the saturation (maximum) stress, m_1 is the rate of isotropic hardening from eq. (11), and

$$K_1 = \left[2 \ln(2D_0 / \sqrt{3}R) \right]^{-(1/2n)} \quad (14a)$$

$$C_1 = (Z_1 - Z_0) / (K_1 Z_0 Z_1) \quad (14b)$$

The usual test condition, however, is control of extension or total strain rate. Equating response behavior for the same plastic and total strain rates at the higher strains seems reasonable but may not be a good approximation at the "knee" of the stress-strain curve, i.e. at stresses slightly above the essentially elastic range. That may be the region of interest for inelastic buckling problems which will be discussed. Numerical solution of the complete set of equations for the uniaxial stress case to obtain a stress-strain curve at a prescribed total strain rate is currently not difficult to perform. The usual engineering yield stress σ_y at 0.2% strain offset can be readily obtained from that curve and would be rate dependent. It follows from eqs. (14,14b) that $\sigma_0 = K_1 Z_0$ where σ_0 is the initial stress level of the stress - fully plastic strain relation, i.e. at $\epsilon^P = 0$. The deduced value σ_0 should be comparable to σ_y so that a practical "yield stress" can therefore be obtained from a theory without a prescribed yield condition.

Equation (11) seems to be the simplest expression for isotropic hardening that provides the principal response characteristics of homogeneous metals. Various modifications based on physical considerations on the microscopic level have been proposed to improve the representational capability, e.g. Estrin and Mecking (1986), but these have not been adequately examined in applications. Alternatively, some modifications have been suggested based directly on enhancing correspondence between simulations and test results for certain metals and for some loading conditions; these are described in the following section.

An important limitation of the isotropic hardening format is its inability to properly represent the response due to changes in the direction of loading. For this purpose, the concept of directional hardening is useful which describes the orientational nature of part of the developed resistance to continued deformation. It would operate primarily on the developed slip planes of the materials and is therefore dependent on stress history and its current value. The so-called Bauschinger effect, which refers to the reduction of hardening upon reversed loading, is the classical example of directional hardening. The terms "anisotropic" and "kinematic" hardening are also used for that purpose but the first is not an accurate use of the word and the second is based on Prager's hardening model of classical plasticity in which a yield surface undergoes rigid body motion in stress space.

A simplistic physical description of directional hardening for single phase pure metals and metallic alloys along the lines of the explanation by Orowan (1959) is that the impediment of dislocation motion on the active slip planes by obstacles, impurities, or other dislocations during the initial loading phase leads, upon reversal of the stress, to enhanced mobility of some of the restrained dislocations in the opposite direction. That is, resistance to dislocation movement is lower for a limited strain excursion in the reversed stress direction. It follows that the strain energy of the local, self-equilibrating stress fields due to the dislocation interactions, the stored energy of cold work (SECW), would be initially reduced by the stress reversal. There seems to be ample experimental evidence for the partial reversibility of dislocations, Sleeswyk et al. (1986), and of the SECW, Halford (1966). Halford confirmed that the reversible action of part of the SECW cannot be due to macroscopic residual stresses but has its origin on the microstructural level.

The actual physics of the material response to reversed stressing is complicated and has been the subject of extensive investigations. As an example, a discussion of detailed dislocation mechanisms that could be responsible for directional hardening was presented by Miller (1987). For two phase metals such as a steel containing a small fraction of dispersed small particles, the internal stress fields due to interactions between the particles and the matrix would also influence the directional hardening properties and the SECW. At large pre-strains, a primary mechanism for softening upon stress reversal could be an alteration in the geometry of the developed dislocation arrangements. Regardless of the detailed mechanisms, the objective on the continuum level is to provide adequate representation of the response characteristics consistent with the underlying physics.

Guided by the above considerations, directional hardening is treated in the proposed constitutive theory as a second order tensor β_{ij} with an evolution equation similar in general form to that of isotropic hardening,

$$\dot{\beta}_{ij}(t) = m_2 [Z_3 u_{ij}(t) - \beta_{ij}(t)] \dot{W}_p(t) - A_2 Z_1 \left\{ \frac{[\beta_{kl}(t) \beta_{kl}(t)]^{1/2}}{Z_1} \right\}^{r_2} v_{ij}(t) \quad (15)$$

where Z_3 is the saturated value of directional hardening, m_2 is the hardening rate, and

$$u_{ij}(t) = \sigma_{ij}(t) / [\sigma_{kl}(t) \sigma_{kl}(t)]^{1/2} \quad (15a)$$

are the direction cosines of the current stress state. Also,

$$v_{ij}(t) = \beta_{ij}(t) / [\beta_{kl}(t)\beta_{kl}(t)]^{1/2} \quad (15b)$$

which indicates that thermal recovery reduces β_{ij} in its current direction, and it has been assumed that there is no initial directional hardening, i.e. $\beta_{ij}(0) = 0$. The maximum isotropic hardening value Z_I is used in eq. (15) only for dimensional purposes. An essential step in the use of eq. (15) in the expression for plastic strain rate, eq. (8), is that a scalar effective value of β_{ij} , namely its amplitude in the direction of current stress u_{ij} ,

$$Z^D = \beta_{ij} u_{ij} \quad (16)$$

is added to the isotropic hardening term Z^I to form a total hardening value,

$$Z = Z^I + Z^D. \quad (16a)$$

In the particular case of uniaxial stress, loading to an initial stress σ_{11} would generate a value for β_{11} . Upon unloading and at the onset of stress reversal, β_{11} would remain essentially unchanged while u_{11} becomes negative or $Z^D = -\beta_{11}$ which reduces the total Z value. In all practical cases, Z^D would be less than Z^I so that Z is always positive. This procedure directly influences the hardening variable and appears to simulate the actual physical process consequent to reversal of stress.

An exercise was performed by Bodner and Lindenfeld (1995) to examine the thermodynamic consistency of the basic equations including those to represent directional hardening. [A related publication is that of Senchenkov and Zhuk (1997).] It was also of interest to compare predictions of the equations to the test results of Halford (1966) on repeated cyclic torsional loading of thin tubes of annealed copper. In particular, Halford measured the detailed changes in SECW during cycling, while the magnitude of the directional hardening variable $|\beta_{ij}|$ in the formulation is intended to be directly related to the potentially reversible part of the SECW upon stress reversal. The correspondence obtained between predictions and test data is good and the sharp drop in SECW upon stress reversal is indicated, Fig. 4.

Repeated load reversals are of particular technological interest and consideration of both isotropic and directional hardening provides the basis for modelling those conditions. For some circumstances, modifications of the hardening evolution equations are required which are discussed in a following section.

An alternative and seemingly more popular method for representing the softening effect upon stress reversal is to identify a state variable α_{ij} , usually termed the "back stress", with the origin of a yield surface in Prager's kinematic hardening model. On that basis, the governing flow law becomes,

$$\dot{\epsilon}_{ij}^P = \lambda' (s_{ij} - \alpha_{ij}) \quad (17)$$

where λ' would be a scalar function of $s_{ij} - \alpha_{ij}$, an isotropic hardening variable Z' , and the temperature. Consequently, the equation for plastic strain rate in the uniaxial stress case can be expressed in the form,

$$\dot{\epsilon}_{11}^P = f(|s_{11} - \alpha_{11}|, Z', T) \text{sgn}(s_{11} - \alpha_{11}) \quad (18)$$

An evolution equation similar to eq. (15) for β_{ij} is usually employed for α_{ij} , which is deviatoric, with differences in the hardening measure and the direction of saturation. In

particular, investigators using eq. (17) generally use an evolution equation that is a more complicated version of the basic form,

$$\begin{aligned} \dot{\alpha}_{ij}(t) = m'_3 [Z'_3 w_{ij}(t) - \alpha_{ij}(t)] \dot{\epsilon}_{\text{eff}}^P(t) \\ - A'_2 Z'_1 \left\{ \frac{[\alpha_{kl}(t)\alpha_{kl}(t)]^{1/2}}{Z'_1} \right\} y_{ij}(t) \end{aligned} \quad (19)$$

where

$$w_{ij}(t) = \dot{\epsilon}_{ij}^P(t) / [\dot{\epsilon}_{kl}^P(t) \dot{\epsilon}_{kl}^P(t)]^{1/2} \quad (19a)$$

$$y_{ij}(t) = \alpha_{ij}(t) / [\alpha_{kl}(t)\alpha_{kl}(t)]^{1/2} \quad (19b)$$

It is seen that the back stress α_{ij} not only provides for the Bauschinger effect but also influences the direction of plastic straining. Most unified theories that utilize the back stress variable are based on an explicit yield criterion and others modify the hardening evolution equations to imply a yield condition. According to Chaboche (1993b), a practitioner of the back stress approach with a yield criterion, the term α_{ij} , like β_{ij} , is directly related to the reversible part of the SECW under reversed stressing conditions. That is, α_{ij} should also represent the macroscopic effect of internal self-equilibrating stress fields on the microscopic level. As a consequence, α_{ij} is more equivalent to a resistance, with the dimension of stress, than an actual macroscopic stress that could, by itself, enter an equilibrium equation. Somewhat similarly, Miller (1987) interprets the resistance corresponding to directional hardening in terms of a "back stress" variable in his formulation. From the viewpoints of mechanics and thermodynamics, the B-P method described in this article of utilizing a directional hardening variable β_{ij} , and the use of a "back stress" variable α_{ij} , are both admissible and essentially correspond to the same physical effect. The choice is primarily in simplicity of application including the identification of the material parameters and in computational efficiency. Formulations based on either procedure in its simplest form generally require modifications or extensions to represent the complexities of actual material behavior. Extensions and applications of the basic equations (8) and (11), with the inclusion of directional hardening according to eqs. (15),(16), are discussed in the following sections.

3. Extensions and Applications of the Basic Equations

3.1 Variable Rate of Hardening/Cyclic Loadings

For the case of uniaxial stress, assumed isotropic hardening with no thermal recovery, and constant plastic strain rate, a specific form of stress-strain curve is obtained given by eq. (14). Some materials such as annealed copper and aluminum exhibit an extensive work hardening region which is not well represented by that equation. To obtain more flexibility and thereby better agreement with test results, a modification was suggested by Bodner et al. (1979) to consider the term m_1 , which controls the hardening rate, to be itself a function of accumulated W_p which introduces two additional material constants,

$$m_1 = a_0 + a_1 \exp(-a_2 W_p) \quad (20)$$

An alternative method based on the current value of the hardening variable Z^I was proposed by Khen and Rubin (1992), namely,

$$m_1 = m_{1b} + (m_{1a} - m_{1b}) \exp[-m_{1c} (Z^I - Z_0)] \quad (21a)$$

with m_{1a} , m_{1b} , m_{1c} being positive constants and Z_0 being the initial value of Z^I . Typically, the value of m_{1a} is larger than m_{1b} so that eq. (21a) causes m_1 to decrease from its initial value of m_{1a} towards the lower value $m_1(Z_1)$ which serves to smoothen the stress-strain curve. A similar modification can be used for the directional hardening rate term m_2 in eq. (15),

$$m_2 = m_{2b} + (m_{2a} - m_{2b}) \exp(-m_{2c} Z^D) \quad (21b)$$

This expression serves to generate a rapid increase in the rate of directional hardening upon stress reversal which is observed in cyclic loading tests. It also tends to smoothen the somewhat "squarish" form of the reversed stress-strain curve. These modifications have been used in a number of applications.

Thermal recovery of hardening can be important at high temperatures and sometimes requires more exact representation than the simple power law expressions used in eqs. (11) and (15). An example is the titanium alloy "Timetal 21S", which is proposed for use in metal matrix composites, where the large rate sensitivity exhibited at 650°C is controlled by thermal recovery of hardening. In this case, it was useful to expand the coefficient A_1 in eq. (11) in a similar manner, as discussed by Neu and Bodner (1995),

$$A_1 = A_{1b} + (A_{1a} - A_{1b}) \exp[-A_{1c} (Z^I - Z_2)] \quad (22)$$

which introduces two more material constants.

The equations described here are capable of adequately representing the Bauschinger effect and reversed loading response especially when variable rates of hardening are introduced, eqs. (21a, 21b). However, stress saturation of cyclic loading due to cyclic hardening or softening may not be well characterized since the same maximum isotropic hardening variable Z_1 applies for both monotonic and cyclic straining. This means there would be a relation between monotonic and cyclic stress-strain curves where the latter is the locus of peak points of saturated loops at different strain amplitudes. Although such a relation seems to exist for some materials, as reported by Chan et al. (1989) for a high temperature alloy, it is not sufficiently general. For representation of repeated cyclic loadings, modification of the evolution equation for the isotropic hardening variable Z^I , which controls the growth or contraction of cyclic stress-strain curves, appears to be necessary. Such a procedure has been developed by Chaboche and co-workers, reported by Chaboche (1993a), using a unified

theory with the "back stress" approach. A similar modification could be adopted to the corresponding equation of the B-P model. Another procedure that provides for the influence of the cyclic loading history on the isotropic hardening variable was suggested by Bodner (1991) but has not been evaluated in applications. Repeated reversed loading conditions with non-zero mean stress could lead to ratchetting for some materials such as stainless steels. It seems that this effect is directly related to directional hardening and that modification of the evolution equation (15) is required. Procedures for doing so have been developed by Ohno and Wang (1993) and more recently by Ohno and colleagues: Mizuno et al. (2000), Ohno and Abdel-Karim (2000).

3.2 Strain Rate Dependence of Hardening Rate

As noted, the basic equations are based on thermal activation of dislocation motion as the primary mechanism governing plastic straining, and the evolution equations for hardening, eq. (11), (15), (16), depend only upon the loading history. However, Klepazco and Chiem (1986) and Estrin and Mecking (1986) and other investigators have indicated that strain rate dependence of the hardening process could be an important factor in the response of fcc metals at moderate and high strain rates. In fact, experiments on annealed pure copper at high strain rates, Follansbee and Kocks (1988) and Tong et al. (1992), indicate strong rate sensitivity of hardening at rates greater than about 10^4sec^{-1} . It was shown by Bodner and Rubin (1994) that, for the case of simple shear and isotropic hardening, a modest modification of the isotropic hardening evolution equation (11) without thermal recovery can serve to provide predictions that are consistent with the available test data.

For annealed copper under shear, eqs. (10) and (11) in conjunction with eq. (21a) were used to obtain compatibility with quasi-static stress-strain test results. At high strain rates, the essential modification was to consider the hardening rate m_I to be also a function of total strain rate by setting m_{Ia} in eq. (21a), the initial value of m_I , to be

$$m_{Ia} = M_a \left[1 + \left(\frac{\dot{\epsilon}_{\text{eff}}}{\dot{\epsilon}_{\text{eff}}^o} \right)^q \right] \quad (23)$$

where $\dot{\epsilon}_{\text{eff}}$ is the effective (deviatoric) total strain rate, eq. (6a) with $\dot{\epsilon}_{ij}^p$ replaced by $\dot{\epsilon}_{ij}$, and $\dot{\epsilon}_{\text{eff}}^o$ and q are additional material constants. A set of material constants consisting of those obtained by matching the quasi-static tests and taking $q=1$ and $\dot{\epsilon}_{\text{eff}}^o$ to be $1 \times 10^4 \text{sec}^{-1}$ was found to give good correspondence with the high strain rate data of Tong et al. (1992), Fig. 5. A feature of the proposed procedure is that the entire relation between the hardening variable Z and plastic work or strain between $Z_0 = 72 \text{ MPa}$ and $Z_I = 920 \text{ MPa}$ is accessible for all imposed strain rates. That is, at slow loading Z_I would only be approached at the larger strains while at high strain rates Z_I will be approached at small strains approximating ideal elastic-perfectly plastic response.

The plot of stress dependence on the logarithm of strain rate for copper at a shear strain of 20% is shown in Fig. 5 [from Bodner and Rubin (1994)]. The lower curve corresponds to constant $Z = 222 \text{ MPa}$ which is the hardening value obtained at the shear strain $\gamma = 0.20$ using the set of material constants that match the low strain rate stress-strain curve. A stress-

strain rate curve for the constant hardening saturation value $Z_1 = 920$ MPa is also shown. Fig. 5 indicates that strain rate dependence of the hardening rate, eq. (23), considerably increases the stress response at the high rates to more rapidly approach the saturation value. A consequence of the hardening rate mechanism is that attempts to model the behavior of copper using only the basic equations and a limited rate range of reference test data could lead to large variations of the strain rate sensitivity parameter n . The modification given by eq. (23) was motivated by test results and implies that the physical basis of the effect is due to changes in the inelastic deformation mechanisms at high strain rates and not in the microstructural configuration at saturation, i.e. Z_1 remains unchanged. This observation may be useful in understanding the physics of inelastic deformation at very high strain rates.

3.3 Creep of metals

For metals, most all creep deformations are permanent, i.e. "inelastic" or "plastic", while a small fraction could be "anelastic" or geometrically reversible. According to Bell (1973), observations of room temperature creep of iron under high constant stress was reported as early as 1830 and measurements of strain with a resolution as low as 10^{-6} were then possible. Modern investigators, however, usually refer to the work of Andrade in 1910 in which some ingenious test arrangements are described and test results are reported for a number of metals. Andrade and later Orowan (1947) suggested an empirical equation for transient (primary) creep strain, $\epsilon^c (= \epsilon_{11}^p)$, as a function of time,

$$\epsilon^c = \epsilon_{11}^p = \beta(t)^{1/3} + c_1 \quad (33)$$

for uniaxial stress conditions. In an important paper at the time, Wyatt (1953) showed that eq. (33) would apply to the transient creep of copper and aluminum at the higher test temperatures (approximately $> 170^\circ\text{C}$) while better matching could be obtained at lower temperatures by a logarithmic function of time,

$$\epsilon^c = \epsilon_{11}^p = \alpha \log t + c_2 \quad (34)$$

which had been proposed by other investigators. The logarithmic function has been shown to be a more generally useful representation. Over the years, other functional forms of transient creep as a function of time have been proposed based on empirical information. However, it should be emphasized that inclusion of explicit time dependence is not appropriate for a generally applicable constitutive equation.

Some investigators have examined the effect of small increments and decrements of stress on the creep response. A few of these studies were directed toward studying the possible applicability of an equation of state of the form $F(\sigma, \epsilon^c, d\epsilon^c / dt, T) = 0$. It was demonstrated by Orowan (1947) that a general equation of state of that form for metals cannot be obtained. This is apparent since $\epsilon^c (= \epsilon_{11}^p)$ is not a state quantity, i.e. it is not representative of the physical state of the material. It seems though that such an equation could serve as an approximation for some limited circumstances such as incremental loading without unloading, e.g. Wyatt (1953).

Steady state (secondary) creep is the condition of constant strain rate under constant stress which is physically attributed to the balance of the rate of hardening and the rate of thermal recovery of hardening (the Bailey-Orowan explanation). The situation could also be realized under imposed straining at a constant rate and leads to constant stress in the stress-strain relation. Steady state would also be obtained by saturation of hardening when thermal recovery is negligible, e.g. at the higher strain rates, or when thermal recovery dominates over hardening effects, e.g. at very low strain rates. In the materials science literature, the steady state creep strain rate is expressed as a function of stress, temperature, and a myriad of quantities that represent overall physical properties and aspects of the microstructure and mesostructure, e.g. grain size, dispersion of particles. Such equations serve as important guides in the development of creep resistant alloys, e.g. Nabarro and Filmer (1993).

The steady state condition, i.e. the steady creep rate, is generally independent of prior creep or straining history and is reasonably reproducible. That is, it is not particularly sensitive to small variations in ingredients or processing procedure. For this reason, better agreement can be obtained by a constitutive theory with steady creep results than with transient creep data. The latter is more subject to details of the initial substructure of the material and to the loading process.

For the structural analyst, it has been traditional to separate time dependent creep effects from the presumed rate-independent stress-strain relation. An example is the BOSOR computer program for shell structures, Bushnell (1985), in which creep directly influences only the geometry of the structure with time. Its effect on the stress state is thereby secondary. This uncoupled plasticity-creep approach may be adequate under certain limited circumstances.

An essential intention of unified constitutive theories is that all inelastic (non-reversible) strains are representable by a single variable. As previously described, creep is the response to a particular loading condition and, for the theory described in this article, is determined by eq. (8) and the associated evolution equations for hardening. In eq. (8), $\dot{\epsilon}_{ij}^p$ is the inelastic strain rate which is a function of stress, temperature, and load history dependent state variables. Specifically, eq. (8) does not contain an explicit function of time, nor does it and the associated hardening evolution equations include plastic strain which is not a state quantity.

The reference constitutive theory has been used in a number of exercises involving creep. Bodner (1979) examined the uniaxial stress behavior of a high temperature alloy, René 95, at a single high temperature (649°C) using the isotropic hardening form with thermal recovery of hardening, eqs. (9) and (11). The test program for the reference data included uniaxial straining with monotonic and cyclic loadings, stress relaxation, and creep. The steady state creep and straining results shown in Fig. 16a indicate three distinct branches. At the test temperature, and the higher strain rates, $\dot{\epsilon}_{11}^p > 10^{-5} \text{ sec}^{-1}$, thermal recovery of hardening was negligible so that steady state resulted from $Z \rightarrow Z_1$ and $\dot{Z} \rightarrow 0$. In the intermediate strain rate range, $10^{-7} - 10^{-5} \text{ sec}^{-1}$, steady state was a consequence of rate balancing in the

hardening evolution equation leading to $\dot{Z} \rightarrow 0$ with corresponding constant inelastic strain rate at constant stress. For the lower strain rates, $< 10^{-7} \text{ sec}^{-1}$, the theory indicated steady strain rates due to dominance of thermal recovery with $Z \rightarrow Z_2$ and $\dot{Z} \rightarrow 0$, where Z_2 is the stable value at a given temperature. Predictions based on the theory were in fairly good agreement with the test results which covered the $\dot{\epsilon}_{11}^P$ range 10^{-8} to 10^{-3} sec^{-1} , Fig. 16a.

A more extensive investigation on creep characteristics based on the B-P theory was performed by Merzer (1982) in relation to reported results on copper. Again, the reference model consisted of eq. (9) with isotropic hardening and thermal recovery of hardening, eq. (11). Test data was available for secondary creep of copper under uniaxial tensile stresses at 550°C over the steady strain rate range of 3×10^{-7} to $4 \times 10^{-4} \text{ sec}^{-1}$, and the model predictions were in fairly good agreement, Fig. 16b. These results covered only the central branch of the stress-strain rate relation but the tendencies at the two ends of the range and computed results indicated similar behavior to that of Fig. 16a. Another exercise performed by Merzer (1982) showed correspondence of the theory with transient creep test results of copper at 200°C . Both sets of results corresponded approximately to eq. (34). The reference theory also seemed capable of demonstrating response characteristics due to stress increments and decrements superimposed on the applied stress.

More recent investigations on the predictive capability of the constitutive theory under multiaxial creep conditions have been reported by Li and Sharpe (1996) and Zeng and Sharpe (1997). Numerical calculations of strains at the roots of notched specimens, based on adopting the constitutive theory to the ABACUS finite element program, were compared to very accurate strain measurements with good correspondence. There seems to be no difficulty in using a unified elastic-viscoplastic model in conjunction with modern finite element and finite difference programs. This is discussed in a subsequent section of this article.

The structural analyst is also challenged with stability problems. Consideration of both nonlinear and time dependent geometrical and material effects can lead to loss of stability which, in some cases, would be directly indicated from the output of the computer program. These instabilities could be caused by the growth of initial structural imperfections, by the increase of deformations due to non-uniform pre-buckling stresses, or by the transition to an unstable geometrical form, such as that of shallow arches of elastic-viscoplastic material [investigated by Simites et al. (1991)]. For some situations, such as the possibility of bifurcation, it may be useful that a stability criterion be injected into the numerical program; this is discussed in a subsequent section on viscoplastic buckling.

3.4 Continuum damage as a state variable

Another quantity representing the material state is the so-called "damage" variable which was introduced by Kachanov (1958), and further developed by Rabotnov (1968), to explain tertiary creep of metals. That refers to the increase of the rate of straining subsequent to secondary creep which leads to material failure. An attempt to define "continuum damage" in a general sense could be based on the postulate of a perfect i.e. undamaged, reference state. With respect to that state, damage could be interpreted as deterioration in the ability of a

material to support stress thereby magnifying the effect of stress on the response. A specific definition of "damage" is elusive but it is often considered to be the presence of geometrical discontinuities in the material such as voids, cracks or debonding of components which reduce the effective load carrying area. These defects are presumed to be small in size compared to the dimensions of the object under discussion but larger than the atomic scale; a level sometimes referred to as the "mesoscale". When the microvoids and microcracks are uniformly distributed and randomly oriented, then damage could be treated as a scalar state quantity. Like hardening, continuum damage is a somewhat abstract concept that intends to represent a definite physical effect without describing the detailed features on the microscopic level. When orientation effects of damage are important, then damage is treated as a second or fourth order tensor which is discussed, for example, by Krajcinovic (1996).

In constitutive equations of the kind discussed here, damage would act to increase both the elastic and inelastic strain rates but the latter seems to be more important for ductile metals. A method for introducing the isotropic damage variable ω in the basic kinetic equation for inelastic straining (8) is to consider it as a softening parameter which decreases resistance to inelastic deformation. On that basis, the hardening variable Z in eq. (8) would be replaced by $Z(1 - \omega)$ where ω can have values from 0 to unity. Attempts have been made to quantify a critical damage value for failure and values ranging from 0.15 to 0.85 for metals have been suggested, Lemaitre (1992).

Inclusion of continuum damage, ω , in the kinetic equation (8) requires specification of an evolution equation for that variable. For the uniaxial stress case, most investigations on the subject employ the general form,

$$\dot{\omega} = f_1(\omega)f_2[\sigma/(1 - \omega)] \quad (24)$$

where f_1 and f_2 are traditionally taken to be power law functions. An alternative expression suggested by Bodner and Chan (1986) for isotropic damage development under multiaxial stress is

$$\dot{\omega} = \frac{p}{H} \left[\ln \left(\frac{1}{\omega} \right) \right]^{(p+1)/p} \omega \dot{Q} \quad (25)$$

where p and H are material constants and $\omega(0) \sim 0$. The assumed multiaxial stress function \dot{Q} suggested by Hayhurst (1972) is,

$$\dot{Q} = [A\sigma_{\max}^+ + B\sigma_{\text{eff}} + CI_1^+]^z \quad (26)$$

where σ_{\max}^+ is the maximum tensile principal stress, I_1^+ is the first stress invariant (positive for tension), σ_{eff} is defined previously, and A , B , C and z are material constants where $A + B + C = 1$.

For the case of constant applied stress, eq. (25) can be integrated to

$$\omega = \exp[-(H/Q)^p] \quad (27)$$

which is the same functional form as the kinetic equation (8) for plastic straining. It was shown by Bodner and Chan (1986) that introduction of the damage variable into the kinetic equation (9), i.e. $Z \rightarrow Z(1 - \omega)$, combined with the damage evolution equations (25), (26) and those for hardening, leads to reasonable agreement with creep test results, including

tertiary creep, for a high temperature alloy. A more thorough analysis and extension of the approach to model creep crack growth was performed by Chan (1988).

As formulated above, damage effects are manifested by the development of tertiary creep, the decrease of the flow stress at moderately high strains under controlled straining, the changes in saturated stress-strain loops under repeated cycling i.e. fatigue, and as the precursor to the onset of cracking at stress concentrations. In principle, damage could also reduce the effective elastic moduli but the changes are usually difficult to measure in metals.

When the damage variable is used in conjunction with constitutive equations such as discussed here, the conditions of plastic incompressibility and pressure independence of plastic flow are usually maintained. For various non-metals such as some crystalline rocks, primary deformation characteristics due to damage are dilation, pressure dependence, and possible damage healing, e.g. Brace et al. (1966). As an example, deformation of a cylindrical specimen of rock salt under sustained axial compression and confining pressure would exhibit pressure dependent dilation due to the formation of wing cracks. If the stress state were readjusted to hydrostatic pressure at some time, then healing of the developed damage and associated strains would take place in two stages. Initially and relatively rapidly, partial closure of the microcracks would occur, followed by slow sintering of adjacent material. Healing of damage does not seem to be a viable process for metals although they do experience thermal recovery of hardening.

A method to treat such effects analytically is to add terms to the flow law, eq. (5), for damage induced straining that indicate dilation and pressure dependence and also for possible damage healing. These would be in addition to the stress enhancement influence of damage, and would correspond physically to the opening of microcracks that leads to dilation and which could be suppressed by the confining pressure. The evolution equations for damage development, eqs. (25), (26), also have to be expanded to include similar effects. Such a formulation was developed for rock salt in a series of papers by Chan et al. (1992,98,99).

An approach to treating damage in the form of voids in ductile materials was developed by Rajendran et al. (1989). In this formulation, the basic response of the void- free matrix material is governed by the B-P equations for which rate dependent plastic flow is isochoric and pressure independent. A revised flow law is obtained by postulating a plastic potential that depends on deviatoric stress, pressure, and the relative density of voids or, correspondingly, the void volume fraction. The flow law associated with that potential function therefore includes dilatation and pressure dependence of inelastic deformation due to the presence of voids. Suitable evolution equations for void nucleation and growth are derived so that a full set of equations for the generation and expansion of voids in a rate dependent ductile matrix is obtained. Material failure develops at high volume fractions of voids due to their coalescence. It is interesting that both the method of Rajendran et al. (1989) for void damage in ductile metals and that of Chan et al. (1992,98,99) for damage in the form of wing cracks in rock salt depend on suitable generalization of the flow law for inelastic deformation.

3.5 Nonproportional loadings

Proportional loading is the condition that the ratios of the respective components of stress, total strain rate, and plastic strain rate remain the same throughout the loading history. From the flow law, eq. (5) and the relation between deviatoric stress, deviatoric total and inelastic strains, eq. (3a), it follows that those tensor variables are co-linear for proportional multi-axial conditions. The constitutive equations described here have generally been found applicable for both proportional and non-proportional loading histories unless the non-proportionality is a major factor of the loading condition.

An example of strong non-proportional loading is the case of a rapid change in the direction of imposed straining in the inelastic range where the interests are the effective modulus (stiffness) at the onset of the change and also the continued response behavior. This case was examined by Rubin and Bodner (1995) and required a generalization of the basic flow law, eq. (5). The matter of effective modulus is directly related to the buckling of structures in the inelastic range when the buckled state exhibits stress components which were previously zero. Another example is the increase of hardening of some metals subjected to repeated cyclic straining by two or more strain components which are out of phase with one another, e.g. Ohno (1990).

The influence of non-proportionality of loading on inelastic response behavior has received attention in recent years. Experiments have indicated changes in the rate of hardening and in the saturation value of hardening of various metals as a consequence of non-proportionality. Methods to provide for these effects have generally been based on proposing a measure of non-proportionality which modifies parameters in the appropriate hardening evolution equations by functions of that measure. Since non-proportionality leads to the generation of additional slip systems, increases of the hardening parameters are usually observed. Proposed measures of non-proportionality are the angles between a pair of the non-dimensional forms of the variables: deviatoric stress, deviatoric stress rate, total deviatoric strain rate, plastic strain rate, and the directional hardening tensor β_{ij} and its rate $\dot{\beta}_{ij}$, e.g. Bodner (1987), Ohno (1990). Other aspects of additional hardening due to non-proportional cyclic loading are described by Doong et al. (1990) and Jinghong and Xianghe (1991).

3.6 Viscoplastic buckling

Criteria for inelastic buckling of ideal structures (without imperfections) by bifurcation, i.e. by the generation of additional deformation modes, have been well established for

rate-independent elastic-plastic materials when the onset of buckling maintains proportional loading conditions. The standard procedure is to replace the elastic modulus in the criterion for elastic buckling by the tangent modulus, i.e. by the tangent to the governing stress-strain curve in the inelastic range at the applicable stress level. For elastic-viscoplastic materials, the mathematical treatment of the bifurcation condition in the inelastic range based on Hill's (1958) stability theory corresponds to requiring an instantaneous jump in strain rate which leads to elastic response and therefore elastic buckling, e.g. Obrecht (1977), Tvergaard, (1989). Inertial effects are not considered in conventional analyses of bifurcation.

That bifurcation of ideal structures of rate dependent materials is elastic is not practically useful and an analytical approach to the problem has been to assume small imperfections in the geometry of the structure in order to determine the maximum load carrying capability from the load-deformation relationship, e.g. Mikkelsen (1993). This method can be reasonably realistic but is cumbersome especially for complicated structures.

Proposals to provide an approximate rate or time dependent tangent modulus from particular response characteristics were made some years ago, e.g. Gerard (1956), Carlson (1956), but these lacked general applicability. These suggestions were based on deducing an effective time and stress dependent tangent modulus from results of tensile creep tests. It is noted, however, that except for the simple cases of linear elasticity and rate independent uniaxial stressing, basic mechanical properties cannot be obtained directly from time dependent response characteristics. The intervention of proper constitutive equations is needed so that the material property could be expressed in terms of state quantities that are load history dependent. Another approach to the creep buckling problem was that of Rabotnov and Shesterikov (1957) who used a dynamic stability criterion based on an equation of motion that included inertial terms and a presumed equation of state for the material. That method was attractive from the basic mechanics viewpoint and led to an expression for a time dependent tangent modulus at the applied stress level which differed from the other formulations. However, their equation of state employed plastic strain which is not a state variable and the predictions were not good.

More recently, Bodner et al. (1991) suggested that an approximate value for the effective tangent modulus for elastic-viscoplastic materials can be obtained in terms of state quantities, particularly, stress and hardening variables. The objective was to use the constitutive model described in this article to obtain an expression for the approximate tangent modulus at bifurcation. From the evolution equations for isotropic and directional hardening, eqs. (11), (15), (16), a plastic tangent modulus can be derived on the basis that the plastic strain rate remains almost constant at buckling and there is also no thermal recovery of hardening. This leads to,

$$E_T^P = [m_1(Z_I - Z^I) + m_2(Z_3 - Z^D)] [\sigma_{\text{eff}}^2 / (Z^I + Z^D)] \quad (28)$$

For general loading conditions, the suggested procedure would be to evaluate σ_{eff} and Z^I and Z^D from the constitutive equations at each increment of loading in order to determine E_T^P from eq. (28). On that basis, a total tangent modulus E_T could be obtained from E_T^P assuming the rate independent relationship, $(1/E_T) = (1/E) + (1/E_T^P)$, which is then used in the rate

independent inelastic buckling criterion. A similar procedure was used by Paley and Aboudi (1991a,b) in their investigations on the inelastic buckling of plates.

For the case of constant stress and the absence of thermal recovery of hardening, eq. (28) indicates a steady decrease of E_T^P and therefore of E_T with continued inelastic straining. As the hardening saturation values Z_1 and Z_3 are approached, E_T would tend to zero indicating, for compressive stress, the possibility of creep buckling. With thermal recovery of hardening considered in the response behavior, eq. (28) implies that creep buckling of a perfect structure could occur only in the primary creep range or not at all. Whether this formulation leads to realistic creep-buckling times has not been examined.

Mikkelsen (1993) compared predictions based on the proposed approximation with load maxima obtained from analyses of columns with initial imperfections under steady total strain rates. A different form of viscoplastic constitutive equation was used in the exercise. The comparisons showed mixed agreements over the range of material rate sensitivity and magnitude of initial imperfection. For some cases, the approximate method led to comparable results. A possible source of the disagreements is that the values used for the stress and the hardening variable in the proposed expression for E_T^P , intended to be equivalent to eq. (28), are based on an overall steady plastic strain rate rather than on a steady total strain rate which would be more realistic for the particular loading circumstance. As discussed previously in relation to eq. (14), the difference in the respective stress-strain curves would be largest at the "knee" of the curves which could be the region of interest for inelastic buckling problems under steadily increasing loading. An alternative procedure for column buckling would be to use the computed stress-strain curve at the relevant steady total strain rate as the reference for obtaining an approximate E_T for "bifurcation".

A recently proposed alternative approach to the stability of structures of rate dependent material is to set up the equations of motion, without inertial effects, for a small perturbation of the system and to establish a linear stability criterion for the response, Massin et al. (1999). This was demonstrated for some simple structures with and without initial imperfections. The application of this approach to practical problems has still to be developed.

An important and more complicated inelastic buckling condition is the development of bifurcation modes with stress components which were zero in the pre-buckled state, i.e. where the onset of buckling leads to non-proportional loading. An example is the case of columns of cruciform cross section that could experience inelastic buckling in torsion (shear) under compressive loading. There are other examples in problems of the inelastic buckling of plates and shells. Classical rate independent, incremental elastic-plastic theory with a yield criterion indicates that such bifurcation modes would respond elastically since there would be zero initial plastic strain rate in the direction of the newly induced stresses. For elastic-viscoplastic materials, non-proportional bifurcation modes would also lead to elastic buckling if the conventional flow law, eq. (5), is employed.

It seems, however, that modification of the flow law could provide a basis whereby an incremental plasticity theory would describe non-proportional buckling involving

viscoplastic materials. Details of the modification and some results are given by Rubin and Bodner (1995) and an outline is presented here.

First, a quantity R_b is introduced which is the reduced effective shear modulus defined as the component of the non-dimensional stress rate in the direction of straining divided by the magnitude of the strain rate, namely,

$$R_b = \left[\left(\frac{\dot{s}_{ij}}{2G\dot{\underline{\epsilon}}} \right) \cdot \left(\frac{\dot{\epsilon}_{ij}}{\dot{\underline{\epsilon}}} \right) \right] = 1 - \left(\frac{\dot{\epsilon}_{ij}^P}{\dot{\underline{\epsilon}}} \right) \cdot \left(\frac{\dot{\epsilon}_{ij}}{\dot{\underline{\epsilon}}} \right) \quad (29)$$

In eq. (29), $\dot{\underline{\epsilon}}$ is the absolute value of the total deviatoric strain rate, $\dot{\underline{\epsilon}} = (\dot{\epsilon}_{ij} \dot{\epsilon}_{ij})^{1/2} \neq 0$, and, from eq. (3c), $\dot{s}_{ij} = 2G(\dot{\epsilon}_{ij} - \dot{\epsilon}_{ij}^P)$ for constant temperature. R_b therefore depends on both the magnitude and direction of the total deviatoric strain rate $\dot{\epsilon}_{ij}$ and the plastic strain rate $\dot{\epsilon}_{ij}^P$. It could be regarded as the non-dimensional tangent shear modulus G_T/G in the direction of the current total deviatoric strain rate. For rate independent material behavior and maintained proportional loading at bifurcation, i.e. $s_{ij}, \dot{\epsilon}_{ij}^P$ and $\dot{\epsilon}_{ij}$ are co-linear, the current tangent modulus would govern buckling, as discussed previously. In relation to eq. (29), bifurcation of ideal structures of rate dependent materials would generate a strain rate jump for which the immediate response would be $\dot{\epsilon}_{ij}^P = 0$ or elastic buckling. It follows that the applicable G_T to control inelastic buckling should be rate independent, such as the suggestion to use the tangent to the current rate dependent stress-strain relation as a rate independent approximation for column buckling.

To further investigate the case of rate dependent material behavior in bifurcation problems involving non-proportional loadings, the plastic flow law, eq. (5), was modified to,

$$\dot{\epsilon}_{ij}^P = \dot{\epsilon}_{ij}^P = \lambda s_{ij} + g(\lambda)F n_{ij} \quad (30)$$

For the added term of eq. (30), n_{ij} is taken to be normal to the current deviatoric stress s_{ij} and to depend directly on the total deviatoric strain rate $\dot{\epsilon}_{ij}$ while the coefficient F is considered to be a non-dimensional function of hardening properties of the material. Also, $g(\lambda)$ acts as the Heavyside function to be unity in the inelastic range. The physical motivation for the addition is to enable immediate generation of plastic flow on the new slip planes activated by the change in direction of the overall strain rate $\dot{\epsilon}_{ij}$. Initial hardening on the newly generated slip planes would be more rapid with increasing strain than continued hardening on the original slip planes, so the physical situation is different from that resulting from bifurcation under proportional loading and is also different than the Bauschinger effect. Similar physical reasoning may have motivated the attempts to justify the deformation theory of plasticity and the concept of corners on a yield surface.

The tensor n_{ij} is assumed to be deviatoric and to be the component of the total deviatoric strain rate normal to deviatoric stress. On that basis,

$$n_{ij} = \dot{\epsilon}_{ij} - (\dot{\epsilon}_{kl} \cdot u'_{kl}) u'_{ij} \quad (31)$$

where u'_{ij} is the direction of deviatoric stress s_{ij} . From eq. (31), the term $g(\lambda)F n_{ij}$ is linear in the total deviatoric strain rate so its contribution to straining would be rate independent. Since n_{ij} is normal to deviatoric stress, the term does not contribute to the plastic work rate. It is non-zero only for non-proportional loading when it acts to modify the elastic strain rate $(\dot{\epsilon}_{ij} - \dot{\epsilon}_{ij}^p)$ and thereby alters the effective modulus. With the modified flow law, the constitutive equations are not in the class of equations considered in previous investigations on viscoplastic buckling and the consequence of elastic buckling at bifurcation does not apply.

In the case of buckling of the compressed cruciform column, it was shown by Rubin and Bodner (1995), that the expression for R_b reduces to $R_b = 1 - F$ at the onset of bifurcation and R_b could vary from close to unity near the beginning of the developed inelastic range and decrease to a value slightly above zero as the hardening prior to buckling approached its fully saturated value. On that basis, F was chosen to be

$$F = k_1 \left[\frac{(\beta_{kl} \beta_{kl})^{1/2}}{Z_3} \right] + k_2 \left[\frac{Z - Z_0}{Z_1 - Z_0} \right], \quad k_1 + k_2 < 1 \quad (32)$$

where $\beta_{kl}(0) = 0$ and $Z(0) = Z_0$. The choices of the constants $k_1 = 0.23$, $k_2 = 0.70$, were found to lead to good agreement with test results on the buckling in torsion of compressed cruciform columns of an aluminum alloy. Expression (32) and the empirical constants, k_1, k_2 have not been confirmed as authentic material properties. Nevertheless, the overall procedure indicates that an incremental elastic-viscoplastic theory without a yield criterion can serve as a possible basis for treating such bifurcation problems.

4. Integration of Constitutive Equations

The basic equations of the unified elastic-viscoplastic theory discussed here consist of the general kinetic equation (8) or a specialized form, eqs. (9) or (10), and the evolution equations for isotropic and directional hardening, eqs. (11), (15), (16). A number of other unified theories of elasto-viscoplasticity have been proposed some of which are described in the volumes edited by Miller (1987), by Freed and Walker (1991) and by Krausz (1996), and reports compiled by Chan et al. (1984) and by Allen and Harris (1990). In view of the potential usefulness of this class of constitutive theories, attention has been given to the problem of numerical integration of the mathematically "stiff" equations inherent in those theories. The intention has been to develop efficient numerical integration schemes that could be adopted into finite element and finite difference programs for the solution of practical problems. One such method was developed by Tanaka and Miller (1988) which was directed toward the constitutive model of Miller [described in Miller (1987)]. Several other computational schemes were examined by Bass and Oden (1988) with reference to a few unified constitutive theories. They proposed a new algorithm which improved the efficiency of the numerical procedures, but relatively large computational times were still required to solve problems.

Some moderately efficient numerical integration schemes were developed directly for use with the B-P constitutive model and were capable of demonstrating the features of load history dependence as well as rate sensitivity, work hardening, and temperature coupling. These included the investigations of Smail and Palazotto (1984) on creep crack growth, Sung and Achenbach (1987) on temperatures generated at a moving crack tip, and that of Dombrowsky (1992). Recently, very efficient methods for integrating the full set of the B-P equations were developed by Rubin (1989) and by Cook, Rajendran and Grove (1992). They used a generalized radial return method together with an implicit integration scheme which, in conjunction with certain general algorithms, lead to short computational runs.

As an example, a computer program for the uniaxial stress σ_{11} case with isotropic and directional hardening, but without thermal recovery of hardening, has been prepared by M.B. Rubin and is included in this article as Appendix A. This specialized integration method is performed in the context of the MATLAB program. Appendix B is a listing of the full nomenclature used in this article.

It is useful to perform a few exercises with this program to demonstrate the capabilities of the equations and the influence of the various parameters on the response characteristics. For the conditions of uniaxial stress, imposed straining and isotropic hardening without thermal recovery, the relevant equations are (9) and the first part of eq. (11). The material constants needed to represent a uniaxial stress-strain relation are E , D_0 , n , Z_0 , Z_1 and m_1 , where E is Young's modulus and D_0 is an assigned quantity. The general shape of the stress-strain curve in the inelastic range obtained at a constant imposed overall strain rate $\dot{\epsilon}_{11}$ is determined by the hardening rate m_1 and the ratio of the saturation to initial hardening variables Z_1/Z_0 , while the particular curve can be obtained by additionally determining Z_0 for a prescribed n , with D_0 initially set. For values of m_1 and Z_1/Z_0 , it is possible from eq. (9) to obtain different combinations of n and Z_0 to represent the same stress-strain curve at a prescribed $\dot{\epsilon}_{11} = \dot{\epsilon}$, as

numerically demonstrated in Fig. 6. For the present exercise, three different values of the parameter n , which controls rate sensitivity of the response, were chosen. Methods for obtaining realistic material constants from test data are described in a subsequent section.

In Fig. 6, three combinations of n and Z_0 , and common values of m_1 and Z_1/Z_0 were used to represent the reference (arbitrarily chosen) stress-strain curve at an imposed strain rate of $\dot{\epsilon}_{11} = \dot{\epsilon} = 10^{-3} \text{ sec}^{-1}$. These sets were:

n	$Z_0(\text{GPa})$	$Z_1(\text{GPa})$	$m_1(1/\text{GPa})$	Z_1/Z_2
0.5	71.35	142.7	50	2
1	10.0	20.0	50	2
5	2.075	4.15	50	2

with $E = 200 \text{ GPa}$ and $D_0 = 10^8 \text{ sec}^{-1}$.

It is of interest to evaluate alternative loading histories that would demonstrate the differing rate sensitivity effects for the various n values. The case of stress relaxation for the three sets of constants is shown in Fig. 7 and the increase of rate sensitivity with decreasing n leads to significantly higher amplitudes of stress relaxation with time. Rate sensitivity effects are even more pronounced for uniaxial straining at imposed rates other than the reference $\dot{\epsilon}_{11} = 10^{-3} \text{ sec}^{-1}$. Simulations for imposed straining rates of 10^{-3} , 1 and 10^3 sec^{-1} are shown in Figs. 8a,b,c for the parameter sets with $n = 5, 1$ and 0.5 respectively. Rate sensitivity of the flow stress for $n = 5$ and associated constants is almost absent while it is pronounced for $n = 0.5$.

A simulation with the set of constants for $n = 1$ was also performed for loading, unloading and reloading at the same high strain rate, $\dot{\epsilon}_{11} = 10^3 \text{ sec}^{-1}$, and is shown in Fig. 9a. Another exercise with initial loading at the high rate but unloading and reloading at the lower rate 1 sec^{-1} is shown in Fig. 9b. The initial unloading response at the lower rate is similar to the stress relaxation process while the reloading flow stress level is lower than the initial stage. However, the memory of the initial high rate loading is maintained in the increased level of the essentially elastic range.

Exercises on rapid changes of strain rate during loading are shown in Figs. 10a,b. A sudden increase of imposed strain rate by 6 decades, 10^{-3} to 10^3 sec^{-1} , is shown in Fig. 10a. The initial elastic response and the approach to the monotonic straining curve at the higher rate are clearly indicated. Alternatively, a sudden six decade decrement in strain rate results in a rapid drop in stress level with respect to strain and an approach to the lower constant strain rate curve from above as seen in Fig. 10b. These realistic features, that the jump to the higher rate is below the constant high rate curve and the jump to the lower rate is above the constant lower rate curve, are consequences of using plastic work, rather than plastic strain rate, in the evolution equation for hardening. There is, however, a time delay between the strain rate reduction and the stress drop as observed experimentally by Lipkin et al. (1978).

As discussed previously, representation of the observed decrease in hardening upon stress reversal requires the introduction of directional hardening described by eqs. (15), (16). Using the set of material constants with $n = 1$ for uniaxial loading, unloading, and continued reversed loading at $\dot{\epsilon}_{11} = 10^{-3} \text{ sec}^{-1}$ provides the solid curve in Fig. 11 based on isotropic hardening. Including directional hardening with rate $m_2 = m_1$ and saturation value $Z_3 = 5$ MPa and reducing that for isotropic hardening Z_1 to 15 MPa (to keep the total hardening at saturation at 20 MPa) leads to the dotted curve in Fig. 11 which is more realistic. Full cyclic response curves are shown in Fig. 12a for isotropic hardening and in Fig. 12b for combined isotropic and directional hardening. The latter is obviously closer to the cyclic behavior of most metals. In many cases, the rate of directional hardening m_2 tends to be more rapid than that for isotropic hardening m_1 . This has the effect, for $m_2 = 3m_1$ in the current exercises, of smoothing the transition from elastic to inelastic behavior, Fig. 13a. Fully reversed cyclic stress-strain curves for $n=1$, $m_2=3m_1$ with isotropic and directional hardening at $\dot{\epsilon}_{11} = 10^{-3} \text{ sec}^{-1}$ are shown in Fig. 13b.

A number of finite element programs have been developed which implement the B-P equations as the material model. These include the following: Newman et al. (1976), [NONSAP] - Zaphir and Bodner (1979), Smail and Palazotto (1984), Dexter et al. (1987), [MARC] - Chan et al. (1989), Pandey et al. (1991), Dexter et al. (1991), Zhu and Cescotto (1991), Dombrovsky (1992), [EPIC-2] - Cook et al. (1992), Nicholas et al. (1993), [ABACUS] - Li and Sharpe (1996), [ABACUS] - Zeng and Sharpe (1997), Kollman and Sansour (1997), Sansour and Kollman (1998). Exercises using the finite difference method with the B-P equations include those of Bodner and Aboudi (1983), Nicholas et al. (1987), and the [STEALTH] code - Rajendran and Grove (1987). The computational results obtained by Bodner and Aboudi (1983) for wave propagation in rods of elastic-viscoplastic are in general agreement with experimental observations as discussed by Nicholas and Rajendran (1990), pp. 133, 134.

5. Material Constants and Applications

5.1 Background

Initial interest in applying unified viscoplastic theories was in determining deformations and stresses in structural components at high temperatures subjected to steady and low frequency cyclic loadings. These problems originated in the operation of gas turbine engines and power generation plants. Strain rates were generally less than 1 sec^{-1} and could be as low as 10^{-7} sec^{-1} . For these problems, the parameter D_0 in the kinetic equation (8) of the B-P model was set to be 10^4 sec^{-1} and sets of material constants were generated on that basis. These applications usually involved high temperatures so thermal recovery of hardening was an important component of the evolution equations. A number of more recent applications of the B-P model were concerned with strain rates above 10 sec^{-1} and were therefore based on the higher value of $D_0 = 10^8 \text{ sec}^{-1}$. These sets of material constants could also be used at lower strain rates making use of modern numerical techniques. Recovery of hardening is usually unimportant in applications at high strain rates so those parameters tend to be omitted in the determination of the high rate material constants.

Some of the early exercises used a slightly different form of the kinetic equation in which the factor $[(n+1)/n]$ appeared as a coefficient to the $(Z^2 / \sigma_{\text{eff}}^2)$ term in equation (8). To correlate all the sets of material constants to the equations described in this article, the parameters Z_0 , Z_1 and Z_2 were re-evaluated in these cases by,

$$Z_0 = [(n+1)/n]^{(1/2n)} \bar{Z}_0, \text{ etc.} \quad (33)$$

where the \bar{Z} values are those given in references with the factor. Values of the other material constants remain unchanged. Those parameter sets with the revalued Z terms are indicated in the following tables by an asterisk. A few other slight variations of the form of the B-P equations used here appear in the literature. For example, Aboudi (1991) employed the above factor and also used (m/Z_0) instead of m_1 in the evolution equation for isotropic hardening eq. (11).

Aside from the matters of the factor in the kinetic equation and the assumed value for D_0 , differences in the derived material constants for presumably the same material are found in some references. One reason is that applications concerned with monotonic loadings tend to use only the isotropic hardening variable and ignore the contribution of directional hardening. This is usually adequate at high strain rates and inelastic strains that are not very small. The influence of the directional hardening variable provides additional flexibility in the representation of monotonic stress-strain relations when used in addition to isotropic hardening and is particularly useful in accurately modelling the region slightly above the primarily elastic range. This was shown in experimental and numerical exercises by Li and Sharpe (1996) and Zeng and Sharpe (1997) to accurately measure and describe the biaxial strains at the roots of notches in axially strained specimens. Another reason for variability is that separate exercises may rely on data bases obtained over different ranges of strain rate which could involve deformation mechanisms in addition to that of thermal activation. This could occur for fcc metals if some of the data is in the range of very high strain rates. Another factor is material variability which is especially characteristic of almost pure metals where small differences in impurities or heat treatment could have a large influence on the

response behavior, e.g. copper and aluminum. Stainless steels also seem to show significant material variabilities, as has been noted by various investigators, which makes them difficult to model.

5.2 Methods for determination of material constants

A few methods of parameter determination from test data for the B-P model have been proposed in the literature. These were based primarily on direct correlation of the influence of the parameters in the equations with particular response characteristics. That is, use was made of the observation that each of the parameters was sensitive to certain information in the appropriate reference test data. In the case of the B-P equations, traditional uniaxial stress tests such as controlled monotonic straining at fixed rates and creep straining at constant stress proved to be adequate for obtaining the parameters in the basic equations.

Conventional tensile, compressive and shear testing can be performed for strain rates up to 1 sec^{-1} while high rates, up to 10^3 sec^{-1} , can be obtained with the Kolsky apparatus - the so-called split Hopkinson bar test (SHB). With special care and analyses, strain rates to 10^4 sec^{-1} have been obtained with the SHB. Higher rates to approximately 10^6 sec^{-1} are achievable with Clifton's apparatus, e.g. Tong et al. (1992). Tests involving rapid changes in strain rates involve complicated strain rate histories and are not recommended as a basis for parameter determination but as examples of possible predictive check tests.

A reasonable test procedure was to perform standard controlled straining tests over a range of applied strain rates and temperatures for which thermal recovery of hardening was negligible. With D_0 initially assigned, the parameters to be determined are n , Z_0, Z_1, Z_3, m_1 and m_2 . Usually, the most influential is n which, for an assigned D_0 , can be obtained from the strain rate dependence of the saturation stress σ_s at which plastic and total strain rates are essentially equivalent under controlled straining. However, most straining tests do not extend to stress saturation because of inelastic instability or test limitations so that condition has to be extrapolated from the available data. Use is made of the general observation that directional hardening saturates more rapidly than isotropic hardening, i.e. $m_2 > m_1$.

The method developed by Chan et al. (1988,89,90a) is to approximate the uniaxial stress-plastic strain curve obtained at a constant total strain rate by taking the stress σ_{11} to be a polynomial function of plastic strain ϵ_{11}^p upon subtracting the elastic strain σ_{11}/E . From this

function, the quantity $\eta = \frac{1}{\sigma_{11}} \frac{d\sigma_{11}}{d\epsilon_{11}^p}$ is evaluated by a least squares method and plotted as a

function of stress. Consistent with the basic equations and for $m_2 > m_1$, such plots are generally bilinear with an upper slope m_2 and a lower slope m_1 as shown in Fig. 14, from Chan et al. (1988). The intercept of the extended curve with $\eta=0$ would be the saturation stress σ_s at which the applied strain rate is equivalent to the plastic strain rate. Performing this exercise at various strain rates would give σ_s as a function of strain rate from which n could be obtained as the slope of the linear plot of the logarithm of the relationship

$(\sigma_s / Z_s) = K_1(\dot{\epsilon}_{11}^P, D_0)$, from eq. (9), with K_1 given by eq. (14a). That slope would be independent of Z_s which is the total hardening value at stress saturation in a monotonic loading test. With n determined, $Z_s = Z_1 + Z_3$ could be obtained from eq. (9) for a particular plastic (total) strain rate and associated stress σ_s at saturation. Another relation involving those parameters and Z_0 corresponds to the intercept of the extension of the upper part of the η - σ plot with $\eta=0$ using the governing equations for that condition. An approximation for obtaining Z_0 would be to use $\sigma_y = \sigma_{11}$ in eq. (9) where σ_y is the engineering yield stress, but here $\dot{\epsilon}_{11}^P$ is not exactly equivalent to the applied $\dot{\epsilon}_{11}$. The approximation could be improved by comparison with the actual stress-strain curves. With Z_0 known, the relations obtained from the η - σ plot serve to determine the individual values of Z_1 and Z_3 . On the basis of this procedure, it is seen that values obtained for n and the hardening constants will depend on the assigned value for D_0 . Changing D_0 would require working through the equations to obtain a new set of constants.

It is noted that the above process enables evaluation of the governing directional hardening parameters, m_2 and Z_3 , from monotonic stress-strain curves. Reversed stressing and cyclic loading curves are generally not required but would be useful checks on the results. In some cases, the monotonic test data may not be adequately sensitive for accurate determination of the directional hardening parameters and reversed stressing tests would then be necessary. When only isotropic hardening is present or when both directional and isotropic hardening have equivalent rates, then the η - σ curve would be linear with a single slope so that consideration of only isotropic hardening would be adequate for modelling purposes.

With the rate sensitivity and hardening parameters determined, creep tests or controlled straining tests at low strain rates provide the information needed to obtain the constants associated with thermal recovery of hardening: A_1, A_2, r_1, r_2 and Z_2 . Details of the procedure are given in Chan et al. (1988,89,90a).

A procedure somewhat similar to that of Chan et al. (1988) was recently developed by Senchenkov and Tabieva (1996) based on numerical integration of the basic equations rather than the plotting of η - σ curves. The authors claim their method is more direct and accurate but in numerical exercises for the same material, a high temperature alloy, the differences of derived parameter values between the two procedures was small.

Another modification to the procedure of Chan et al. (1988) was exercised by Rowley and Thornton (1996) in obtaining sets of B-P material constants for Hastelloy-X and Aluminum alloy 8009. The proposed method involves assuming an initial value for n , obtaining the corresponding hardening constants, and then refining the values by an iteration procedure. The matching of the resulting stress-strain simulations to the test data was very good over a range of strain rates and temperatures.

Applying the method of Chan et al. (1988) to test results for a ductile steel, A533B, obtained over a large range of strain rates, 10^{-3} to 10^3 sec^{-1} , and temperatures, -60 to 175°C ,

indicated that using only isotropic hardening was adequate in this case, Dexter and Chan (1990). The η - σ curves for this material were essentially linear until saturation. All the material constants were evaluated in a straightforward manner and thermal recovery of hardening was not operative over the ranges of interest.

Another series of tests at high strain rates, $100 - 2000 \text{ sec}^{-1}$ using the SHB and also some plate impact tests at higher rates, was performed by Rajendran et al. (1986) [see also Cook et al. (1992)]. Test results extended to saturation but details at the "knee" of the stress-strain curves were lacking. For the intended purpose of analyzing structures under impact loadings that generated moderate strain levels, it seemed that only isotropic hardening without thermal recovery would be sufficient. With D_0 fixed at 10^8 sec^{-1} , the parameters to be determined were n, Z_0, Z_1, m_1 , and $\dot{\epsilon}_{11}^p$ was assumed to be equivalent to $\dot{\epsilon}_{11}$ over the inelastic range of interest. A slightly different parameter determination procedure than that of Chan et al. (1988) was used in that exercise, [Rajendran et al. (1986)]. As in the procedure of Chan et al., n was determined from the strain rate dependence of the saturation stress. Eq. (9) was rewritten in terms of logarithmic functions so it could be represented as a linear relation with slope $-2n$. The test results were plotted to the same stress-strain rate coordinates which enabled determination of the material constants n and Z_1 . The values of m_1 and Z_0 were subsequently obtained by fitting the test results to the integrated form of the evolution equation for isotropic hardening, eq. (11) without thermal recovery, i.e. eq. (12).

It is noted that the methods for parameter determination described above involve step by step procedures so that the results are not necessarily unique but have been found suitable for practical purposes. More sophisticated methods for identification of material constants have been developed by Mahnken and Stein (1996) and by Senseny and Fossum (1995) and Fossum (1998). These should lead to unique parameter values but are somewhat complicated to use. However, they could serve as a means of refinement of the parameter values obtained by the methods based on physical interpretations.

Sets of material constants based on the reference constitutive theory have been published for a number of metals and metallic alloys. Some of these sets are listed in the following section and their probable ranges of applicability are indicated. In the few cases of variations in the obtained constants for the same material, the author has listed what he considers to be the most reliable sets of values presently available.

5.3 Examples

5.3.1 A. Alloys for high temperature applications at low strain rates; assumed

$$D_0 = 10^4 \text{ sec}^{-1}.$$

5.3.1. B1900 +Hf, a Nibase alloy:

5.3.1.1.1 Non-Creep Characterisitcs

References: Chan et al. (1988, 1989, 1990a,b).

Temperature Range: RT to 1093°C.

Strain Rates: 10^{-8} to $5 \times 10^{-3} \text{ sec}^{-1}$.

Considered Applicable Strain Rate Range: 10^{-8} to 10^1 sec^{-1} .

Conditions: uniaxial and biaxial tensile, creep and cyclic under proportional and non-proportional loading, thermomechanical loading paths, and isotropic and directional hardening with thermal recovery.

Temperature-Independent Constants: $D_0 = 10^4 \text{ sec}^{-1}$,

$Z_1 = 3000 \text{ MPa}$, $Z_3 = 1150 \text{ MPa}$, $m_1 = .270 \text{ MPa}^{-1}$, $m_2 = 1.52 \text{ MPa}^{-1}$, $r_1 = r_2 = 2$

temperature dependent constants:

Constants	Temperature, °C			
	$T \leq 760^\circ\text{C}$	871°C	982°C	1093°C
n	1.055	1.03	0.85	0.70
$Z_0 (=Z_2) \text{ (MPa)}$	2700	2400	1900	1200
$A_1=A_2(\text{sec}^{-1})$	0	.0055	.02	.25

Elastic Moduli for B1900+Hf:

$$E = 1.987 \times 10^5 + 16.78 T - .1034 T^2 + 1.143 \times 10^{-5} T^3 \text{ MPa with } T \text{ in } ^\circ\text{C}$$

$$G = 8.650 \times 10^4 - 17.58 T + 2.321 \times 10^{-2} T^2 - 3.464 \times 10^{-5} T^3 \text{ MPa with } T \text{ in } ^\circ\text{C}$$

Note: this metal does not experience additional hardening under non-proportional biaxial cycling.

5.3.1.1.2 B1900+Hf - creep damage investigation, tertiary creep, creep crack growth:

References: [Bodner and Chan (1986), Chan (1988)].

Temperature Range: 649°C to 1093°C.

Strain Rates: 10^{-8} to $5 \times 10^{-3} \text{ sec}^{-1}$.

Considered Applicable Strain Rate Range: 10^{-8} to 10^1 sec^{-1} .

Conditions: uniaxial tensile straining and constant load tensile creep, isotropic and directional hardening with thermal recovery and isotropic damage development.

Temperature-Independent Constants for Damage Development, eqs. (22,23):

$p = 1$, $z = 8.34$, $\omega_0 = 1 \times 10^{-9}$, in addition to previously listed constants.

Temperature Dependent Damage Constant, eq. (22):

$$H[(\text{MPa})^z \text{ sec}] = 2 \times 10^{27} (871^\circ\text{C}); 4 \times 10^{24} (982^\circ\text{C}); 5 \times 10^{20} (1093^\circ\text{C})$$

5.3.1.2 René 95:

Reference: [Bodner (1979)].

Temperature Range in Above Reference: at 650°C only.

Strain Rates in Above Reference: 10^{-8} to 10^{-3} sec^{-1} .

Considered Applicable Strain Rate Range: 10^{-8} to 10^1 sec^{-1} .

Conditions: uniaxial monotonic and cyclic straining and creep and stress relaxation, isotropic hardening with thermal recovery.

Material Constants (650°C): $D_0 = 10^4 \text{ sec}^{-1}$,

$n = 3.2$, $Z_0 (= Z_2) = 1670 \text{ MPa}$, $Z_1 = 2300 \text{ MPa}$, $m_1 = 0.4 \text{ MPa}^{-1}$,

$A_1 = 4 \times 10^{-4} \text{ sec}^{-1}$, $r_1 = 1.5$, $E = 1.77 \times 10^5 \text{ MPa}$.

Where Z is revalued for factor in kinetic equation

5.3.1.3 IN-100:

References: [Smail and Palazotto (1984), from Stouffer (1981)].

Temperature Range in Above References: at 732°C only.

Strain Rates in Above References: 10^{-8} to 10^{-3} sec^{-1} .

Considered Applicable Strain Rate Range: 10^{-8} to 10^1 sec^{-1} .

Conditions: uniaxial monotonic and cyclic straining and creep, isotropic hardening with thermal recovery, investigation of creep crack growth in compact tension specimens.

Material Constants (732°C): $D_0 = 10^4 \text{ sec}^{-1}$,

$n = 0.7$, $Z_0 = 11,880 \text{ MPa}$, $Z_1 = 13,180 \text{ MPa}$, $Z_2 = 7800 \text{ MPa}$,

$m_1 = 0.37 \text{ MPa}^{-1}$, $A_1 = 1.9 \times 10^{-3} \text{ sec}^{-1}$, $r_1 = 2.66$, $E = 1.793 \times 10^5 \text{ MPa}$

Where Z is revalued for factor in kinetic equation

5.3.1.4 Inconel 718:

This material has received attention because of its high temperature applicability but is difficult to model in certain temperature and strain rate ranges where it exhibits dynamic strain ageing and consequently negative strain rate sensitivity. That was demonstrated by James et al. (1987) for tests at 593°C and an empirical correction factor formulated by Schmidt and Miller was introduced for adequate representations of the results. Other test programs were performed at 650°C with associated exercises on the determination of parameters considering isotropic hardening with thermal recovery of hardening, Eftis et al. (1989), Kolkailah and McPhate (1990). What seems to be the most exacting series of tests at 650°C were carried out more recently by Li and Sharpe (1996) and the parameter determination procedure considered both isotropic and directional hardening and their thermal recovery. The B-P equations with those parameters were then used to predict stresses, strains and deformations at the roots of notched specimens under monotonic and cyclic loadings and under creep conditions. Comparisons of the predicted biaxial strains to accurate optical measurements at the notch roots indicated very good agreement.

Reference: [Li and Sharpe (1996)].

Temperature Range: at 650°C only.

Strain Rates: 10^{-7} to $5 \times 10^{-4} \text{ sec}^{-1}$; dynamic strain ageing appeared at $\dot{\epsilon} \geq 10^{-3} \text{ sec}^{-1}$.

Conditions: at 650°C, uniaxial and cyclic straining and constant load tensile creep, isotropic and directional hardening with thermal recovery.

Material Constants (650°C): $D_0 = 10^4 \text{ sec}^{-1}$, $n = 1.12$, $Z_0 (= Z_2) = 5000 \text{ MPa}$,

$Z_1 = 6000 \text{ MPa}$, $Z_3 = 660 \text{ MPa}$, $m_1 = 0.046 \text{ MPa}^{-1}$, $m_2 = 0.84 \text{ MPa}^{-1}$,

$A_1 = A_2 = 3.4 \times 10^{-2} \text{ sec}^{-1}$, $r_1 = r_2 = 6.7$. $E = 175.0 \text{ GPa}$.

5.3.1.5 Hastelloy-X:

Reference: Rowley and Thornton (1996).

Temperature Range: RT (25°C) to 538°C.

Strain Rates: 2×10^{-5} to $2 \times 10^{-3} \text{ sec}^{-1}$.

Considered Applicable Strain Rate Range: 10^{-7} to 10^0 sec^{-1} .

Conditions: uniaxial tensile, no thermal recovery in test temperature range.

Temperature-Independent Constants: $D_0 = 10^4 \text{ sec}^{-1}$,

$Z_1 = 2390 \text{ MPa}$, $Z_3 = 603 \text{ MPa}$, $m_1 = 0.139 \text{ MPa}^{-1}$, $m_2 = 3.49 \text{ MPa}^{-1}$

Table 3. Temperature Dependent Constants:

<u>Constants</u>	<u>Temperature, °C</u>			
	<u>T=25°C</u>	<u>204°C</u>	<u>371°C</u>	<u>538°C</u>
n	1.00	0.90	0.85	0.824
$Z_0 (=Z_2)$ (MPa)	1860	1830	1790	1760
E(GPa)	197	187	175	161

5.3.1.6 Astroloy:

Reference: Dexter, Chan and Coutts (1991).

Temperature Range: RT (25°C) to 982°C.

Strain Rates: 5×10^{-6} to $1 \times 10^{-3} \text{ sec}^{-1}$.

Considered Applicable Strain Rate Range: 10^{-7} to 10^0 sec^{-1} .

Conditions: tensile straining and constant load creep, isotropic hardening with thermal recovery.

Temperature-Independent Constants: $D_0 = 10^4 \text{ sec}^{-1}$,

$Z_1 = 29000 \text{ MPa}$, $r_1 = 2$.

Temperature-Dependent Constants:

Constants	Temperature, °C			
	T=25°C	760°C	871°C	982°C
n	0.524	0.509	0.456	0.387
$Z_0 (=Z_2) \text{ (MPa)}$	23,000	23,000	21,000	20,000
$m_1 \text{ (MPa}^{-1})$	0.015	0.320	0.320	0.675
$A_1 \text{ (sec}^{-1})$	0	0	4×10^{-3}	-
E(GPa)	220	163	149	118

5.3.2 *Applications at low strain rates ($< 10 \text{ sec}^{-1}$); assumed $D_0 = 10^4 \text{ sec}^{-1}$*

5.3.2.1 High Purity Aluminum (99.9999):

Reference: Mahnken and Stein (1996).

Temperature Range: at 277°C only.

Strain Rates: 5×10^{-6} to $2 \times 10^{-4} \text{ sec}^{-1}$.

Considered Applicable Strain Rate Range: 5×10^{-6} to 10^{-3} sec^{-1} .

Conditions: uniaxial tensile straining and creep, isotropic hardening only with no thermal recovery.

Material Constants (277°C): $D_0 = 10^4 \text{ sec}^{-1}$,

$n = 1.38$, $Z_0 = 1380 \text{ MPa}$, $Z_1 = 2860 \text{ MPa}$, $m_1 = 3.8 \text{ MPa}^{-1}$

Where Z is revalued for factor in kinetic equation

5.3.2.2 Aluminum Alloy 8009

Reference: Rowley and Thornton (1996)

Temperature Range: 25#°C to 275#°C.

Strain Rates: 10^{-7} to $5 \times 10^{-3} \text{ sec}^{-1}$.

Considered Applicable Strain Rate Range: 10^{-7} to 10^{-2} sec^{-1} .

Conditions: uniaxial compressive straining and tensile creep, isotropic and directional hardening with thermal recovery.

Temperature Independent Constants: $D_0 = 10^4 \text{ sec}^{-1}$,

$Z_1 = 937 \text{ MPa}$, $Z_3 = 275 \text{ MPa}$, $m_1 = 0.532 \text{ MPa}^{-1}$, $m_2 = 3.95 \text{ MPa}^{-1}$

Temperature Dependent Constants for Aluminum Alloy 8009

<i>Constants</i>	<u>25#°C</u>	<u>100#°C</u>	<u>175#°C</u>	<u>225#°C</u>	<u>275#°C</u>
n	1.95	1.72	1.64	1.47	1.35
$Z_0 (= Z_2) \text{ MPa}$	828	793	758	724	690
$A_1 (\text{sec}^{-1})$	0	0	0.02	0.03	0.05
$r_1 = r_2$	-	-	3	3	3
E(GPa)	83.4	79.3	69.0	67.5	65.5

5.3.2.3 Aluminum Alloy AMG-6 (Russian)

Reference: [Senchenkov and Tabieva (1996)].

Temperature Range: 20#°C to 400#°C.

Strain Rates: $10^{-7} - 4 \times 10^{-2} \text{ sec}^{-1}$.

Considered Applicable Strain Rate Range: 10^{-7} to 10^{-1} sec^{-1} .

Conditions: tensile straining, isotropic and directional hardening with thermal recovery.

Temperature-Independent Constants: $D_0 = 10^4 \text{ sec}^{-1}$,

$Z_1 = 647 \text{ MPa}$, $Z_2 = 35 \text{ MPa}$, $Z_3 = 80 \text{ MPa}$,

$m_1 = 0.182 \text{ MPa}^{-1}$, $m_2 = 3.7 \text{ MPa}^{-1}$, $r_1 = r_2 = 4$.

Temperature-Dependent Constants for Aluminum Alloys

<i>Constants</i>	<u>20#°C</u>	<u>300#°C</u>	<u>400#°C</u>
n	2.06	2.0	1.9
Z_0 (MPa)	324	306	280
A_1 (sec ⁻¹)	0	3.5×10^{-3}	0.15
A_2 (sec ⁻¹)	0	5.4×10^{-2}	0.99

5.3.2.4 Zirconium Alloy (Zr - 2.5 wt percent Nb)

Reference: [Zeng and Sharpe (1997)].

Temperature Range: at 250#°C only.

Strain Rates: $10^{-8} - 10^{-3} \text{ sec}^{-1}$.

Considered Applicable Strain Rate Range: 10^{-8} to 10^{-1} sec^{-1} .

Conditions: uniaxial tensile straining and creep, isotropic and directional hardening with thermal recovery.

Material Constants (250#°C): $D_0 = 10^4 \text{ sec}^{-1}$,

$n = 3.2$, $Z_0 (= Z_2) = 825 \text{ MPa}$, $Z_1 = 916 \text{ MPa}$, $Z_3 = 230 \text{ MPa}$.

$m_1 = 0.06 \text{ MPa}^{-1}$, $m_2 = 1.8 \text{ MPa}^{-1}$, $A_1 = A_2 = 10^{-7} \text{ sec}^{-1}$, $r_1 = r_2 = 2.2$.

$E = 95 \text{ GPa}$, $\nu = 0.3$.

Notes: The above material parameters were used in the B-P theory to predict biaxial strains at the roots of notched specimens during loading and for a creep duration of 100 hours. Comparisons with accurate optical measurements indicated very good agreement.

5.3.2.5 Eutectic Solder, 63/37 Sn/Pb:

Reference: [Skipor, Harren and Botsis (1996)].

Temperature Range: -40#°C to 100#°C.

Strain Rates: 7×10^{-10} to 10^{-1} sec^{-1} .

Considered Applicable Strain Rate Range: 10^{-9} to 10^{-1} sec^{-1} .

Conditions: tensile straining and steady load creep, isotropic hardening with thermal recovery.

Temperature-Independent constants (in above temperature range): $D_0 = 10^4 \text{ sec}^{-1}$,

$Z_0 (= Z_2) = 1550 \text{ MPa}$, $Z_1 = 1900 \text{ MPa}$, $m_1 = 0.90 \text{ MPa}^{-1}$

Temperature-Dependent Constants:

<i>Constants</i>	<u>-40#°C</u>	<u>-10#°C</u>	<u>20#°C</u>	<u>60#°C</u>	<u>100#°C</u>
n	0.475	0.445	0.439	0.412	0.391
$A_1 (\text{sec}^{-1})$	0	1.12×10^{-5}	5.1×10^{-3}	8.6×10^{-3}	4.1×10^9
r_1	-	1.2	1.9	2.3	8.5
E(GPa)	32	27	20	16	12

5.3.2.6 Titanium Alloy Timetal 21S (a candidate matrix material for a MMC):

Reference: Neu and Bodner (1995).

Temperature Range: at 482#°C and at 650#°C.

Strain Rates: 10^{-6} - 10^{-3} sec⁻¹.

Considered Applicable Strain Rate Range: 10^{-7} to 10^{-2} sec⁻¹.

Conditions: tensile straining and creep, isotropic and directional hardening with thermal recovery.

Temperature-Independent Constants (for the Two Temperatures Indicated):

$$D_0 = 10^4 \text{ sec}^{-1},$$

$$Z_1 = 3500 \text{ MPa}, Z_3 = 100 \text{ MPa}$$

$$* m_{1a} = 20 \text{ MPa}^{-1}, * m_{1b} = 2.0 \text{ MPa}^{-1}, * m_{1c} = 0.001 \text{ MPa}^{-1}$$

$$m_2 = 4.0 \text{ MPa}^{-1}$$

$$** A_{1b} = 2 \times 10^{-4} \text{ sec}^{-1}, ** A_{1c} = 0.005 \text{ MPa}^{-1}$$

$$A_2 = 2 \times 10^{-4} \text{ sec}^{-1}, r_1 = r_2 = 3.5$$

Temperature-Dependent Constants for Timetal 21S:

<i>Constants</i>	<u>482#°C</u>	<u>650#°C</u>
n	1.15	0.94
$Z_0 (= Z_2)(\text{MPa})$	300	100
$** A_{1a} (\text{sec}^{-1})$	0.01	100

* Defined by eq. (21a)

** Defined by eq. (22)

5.3.3 Applications at high strain rates ($> 10 \text{ sec}^{-1}$); assumed $D_0 = 10^8 \text{ sec}^{-1}$.

5.3.3.1 References: results obtained by Rajendran, Bless and Dawicke (1986) for a number of metals; also published in Nicholas and Rajendran (1990) page 208; Cook et al. (1992), and Zukas (1994) page 10.

Strain Rates: 10^2 to $3 \times 10^3 \text{ sec}^{-1}$.

Considered Applicable Strain Rate Range: 10 to 10^4 sec^{-1} .

Conditions: room temperature only, isotropic hardening with no thermal recovery.

material constants, room temperature: $D_0 = 10^8 \text{ sec}^{-1}$.

material	n	*M	**Z ₀ (MPa)	**Z ₁ (MPa)	m ₁ (MPa ⁻¹)
C1008 steel	0.4	4.787	26,330	33,500	0.015
HY100 steel	1.2	1.287	3,090	4,570	0.01
1020 steel	4.0	1.028	658	956	0.03
6061-T6 alum.	4.0	1.028	463	565	0.12
7039-T64 alum.	4.0	1.028	576	780	0.028
Nickel 200	4.0	1.028	330	843	0.04
W2 - tungsten	0.58	2.372	20,760	23,720	0.15
Armco iron	0.58	2.372	6,275	9,960	0.056

Notes: The values of Z_0 , Z_1 in the table on p.208 of Nicholas and Rajendran (1990) are based on the factor $[(n+1)/n]$ in the kinetic equation although their statement of the kinetic equation, eq. (96), is equivalent to eq. (8) of this article; a misprint exists in the printing of the B-P kinetic equation of Zukas (1994), p.10, but the table of the B-P model constants appears to be consistent with those with the factor.

Values of constants Z_0 , Z_1 revalued according to eq. (33) to conform to equations (8) and (11) in this report (**).

*M: Multiplier for reevaluation of Z_0 and Z_1 from reference data.

** Z is revalued for factor in kinetic equation

5.3.3.2 Alpha Titanium (Commercially Pure):

Reference: Gilat and Tsai (1990).

Temperature Range: room temperature only.

Strain Rates (data taken from different sources): 10 to 10^3 sec^{-1} .

Considered Applicable Strain Rate Range: 10 to 10^4 sec^{-1} .

Conditions: dynamic shear tests, isotropic and directional hardening without thermal recovery.

Material Constants (room temperature): $D_0 = 10^8 \text{ sec}^{-1}$,

$n = 0.708$, $Z_0 = 5063 \text{ MPa}$, $Z_1 = 5740 \text{ MPa}$, $Z_3 = 380 \text{ MPa}$,

$m_1 = 0.034 \text{ MPa}^{-1}$, $m_2 = 0.520 \text{ MPa}^{-1}$,

$E = 118 \text{ GPa}$, $\nu = 0.34$ (other sources).

5.3.4. Applications over a wide range of strain rates (10^{-4} to 10^6 sec^{-1}); assumed
 $D_0 = 10^8 \text{ sec}^{-1}$.

5.3.4.1 Pure Copper (99.99%)

5.3.4.1.1 OFE for the lower strain rates, OFHC for the high rates.

Main Reference: Bodner and Rubin (1994).

Strain Rates (in shear): 10^{-4} to 10^6 sec^{-1} .

Conditions: uniaxial shear over a wide range of strain rates at room temperature, isotropic hardening without thermal recovery.

Material Constants (room temperature):

$D_0 = 5 \times 10^7 \text{ sec}^{-1}$, $n = 3.4$, $Z_0 = 72 \text{ MPa}$, $Z_1 = 920 \text{ MPa}$,

$^{**}M_a = 36 \times 10^{-3} \text{ Mpa}^{-1}$, $^{*}m_b = 0.5 \times 10^{-3} \text{ MPa}^{-1}$, $^{*}m_c = 7.0 \times 10^{-3} \text{ MPa}^{-1}$,

$^{**}\dot{\epsilon}_{\text{eff}}^0 = 1 \times 10^4 \text{ sec}^{-1}$, $^{**}q = 1.0$,

** defined by eqs. (21a), (23)

* defined by eq. (21a)

Notes: Stress-strain rate results are shown in Fig. 5 of this report. Studies on creep of copper at high temperature were performed by Merzer (1982). An exercise on temperature dependence of the uniaxial stress-strain curves of copper at a constant strain rate is summarized on the following page.

5.3.4.1.2 Pure Copper (99.99%).

Main Reference: Bodner and Rajendran (1996).

Strain Rate (in Compression): 2000 sec^{-1} .

Conditions: uniaxial compression over a wide temperature range (RT to 800°C) at a single strain rate (2000 sec^{-1}), isotropic hardening with temperature dependence of the saturated hardening variable Z_1 .

Temperature-Independent Material Constants:

$$D_0 = 5 \times 10^7 \text{ sec}^{-1}, \quad n = 3.4, \quad Z_0 = 40 \text{ MPa},$$

$$**M_a = 36 \times 10^{-3} \text{ Mpa}^{-1}, \quad *m_b = 3.6 \times 10^{-3} \text{ MPa}^{-1}, \quad *m_c = 7.0 \text{ MPa}^{-1},$$

$$**\dot{\epsilon}_{\text{eff}}^0 = 1 \times 10^4 \text{ sec}^{-1}, \quad **q = 1.0,$$

** defined by eqs. (21a), (23)

* defined by eq. (21a)

Bilinear temperature dependence of $Z_1(T)$ [$Z_1(T_0) = 1450 \text{ MPa}$] is as follows:

$$Z_1 \rightarrow Z_1 \left(1 - \left[\frac{T - T_0}{\bar{T} - T_0} \right]^d \right) \quad ; \quad T < T_t \text{ (transition temperature)}$$

(\bar{T} determines slope of $Z_1(T)$ for $T < T_t$,
it is not a physical value)

$$Z_1 \rightarrow Z_1 \left(1 - \left[\frac{T - T_t}{T_m - T_t} \right]^d \right) \quad ; \quad T \geq T_t,$$

$$\text{where } d = 1, \quad T_0 = 25^\circ\text{C}, \quad T_t = 850^\circ\text{C}, \quad T_m = 1083^\circ\text{C}, \quad \bar{T} = 1450^\circ\text{C}$$

Note: Measured compressive stress-strain curves for copper over the temperature range RT to 800°C at the imposed strain rate of 2000 sec^{-1} and corresponding simulations are shown in Figure 15.

5.3.4.2 Annealed Commercially Pure Aluminum, 1100-0:

Reference: Huang and Khan (1992).

Strain Rates: $10^{-5} - 10^4 \text{ sec}^{-1}$.

Temperature Range: RT only.

Conditions: uniaxial compression testing at room temperature over a wide range of strain rates, isotropic hardening only without thermal recovery.

Material Constants (Room Temperature) for Strain Rate Range; 10^{-5} to $4 \times 10^3 \text{ sec}^{-1}$:

$$D_0 = 10^8 \text{ sec}^{-1}, n = 0.87, Z_0 = 550 \text{ MPa}, Z_1 = 1030 \text{ MPa}$$

$$m_1 = (m'/Z_0) \times 10^2 = 4 \times 10^{-4} \text{ MPa}^{-1}.$$

Notes: This reference indicates good agreement of simulations based on the isotropic hardening B-P model with the performed tests over most, but not all, of the range of results; primary disagreements were as follows:

(a) regions of stress-strain curves slightly beyond the essentially elastic range were not well represented; this was apparently due to the non-inclusion of directional hardening, equations (15 and 16) as was used for the modeling of aluminum alloys, pages 61, and 62.

(b) apparent need for different values for n at slow and high strain rates; this seems to be due to the noninclusion of the strain rate dependence of the hardening rate at the high strain rates, equation (23), as was used for modeling copper, page 68.

5.3.4.3 A533B Steel:

Reference: Dexter and Chan (1990).

Temperature Range in above reference: -60#°C to 175#°C.

Strain Rates in above reference: 10^{-3} to 10^3 sec^{-1} .

Considered Applicable Strain Rate Range: 10^{-4} to 10^4 sec^{-1} .

Conditions: tensile testing over a range of strain rates and temperature, isotropic hardening without thermal recovery.

Temperature Independent Material Constants (over range of interest):

$$D_0 = 10^8 \text{ sec}^{-1}, E(RT) = 207 \text{ GPa}.$$

Temperature Dependent Material Constants for A533 B Steel

<u>Constants</u>	<u>-60#°C</u>	<u>-10#°C</u>	<u>50#°C</u>	<u>100#°C</u>	<u>175#°C</u>
n	1.62	1.68	1.75	2.57	2.77
Z ₀ (MPa)	1772	1491	1379	907	827
Z ₁ (MPa)	2224	1992	1804	1236	1112
m ₁ (MPa ⁻¹)	.050	.053	.064	.066	.074

Note: Unlike most metals, strain rate sensitivity decreases with increasing temperature (n becomes larger); as the authors point out, this may be due to dynamic strain-aging at the higher temperatures. However, the flow stress at a given plastic strain does decrease with increasing temperature, as expected, since the decrease of hardening (Z₀, Z₁) with temperature appears to have a stronger influence on the flow stress than that of the increase of the rate sensitivity parameter n.

6. Further Developments

6.1 Large Deformations

A number of formulations of rate-independent and rate-dependent plasticity for large deformations have been proposed in recent years. An early contribution for rate dependent materials was that of Bodner and Partom (1972b). There is still controversy as to which formulation is most appropriate, but the one most relevant to the constitutive equations described in this report is that of Rubin (1986). A feature of that large strain theory is that all the material constants are obtainable from the corresponding set of small strain equations described here. That is, no additional material constants are required when large deformations are considered. The theory also seems to be free of non-physical peculiarities that rise in some other proposals. Another recent formulation of a large deformation theory is due to Sansour and Kollman (1997,98).

An essential difficulty in assessing large deformation theories of plasticity is the lack of experimental data that is sensitive to the different formulations. The design and performance of such experiments would seem to be a reasonable objective for future investigations.

6.2 Anisotropic materials

Of considerable interest are fiber-matrix composites in which one or more components are elastic-viscoplastic. There seem to be two general approaches in modelling the mechanical behavior of these anisotropic materials. One is to perform a detailed analysis of a typical sub-volume in which the distinct geometries of the fibers and matrix are evident and distinguishable so that the response of the mini-structure to loading can be treated as a mechanics problem. This micro-mechanics or meso-mechanics approach, as it is sometimes called, has received much attention. One example is the "method of cells" developed by Aboudi (1991). In some of the applications of this method, the matrix is considered to be elastic-viscoplastic governed by the B-P equations while the fibers are taken to be elastic and are isotropic or transversely isotropic. Apparent advantages of the B-P equations in this application are the lack of a yield condition and the capability of treating both plastic deformation and creep by the same set of equations.

Other procedures using analyses on the microscale have been developed based on the finite element method. Some of these have also incorporated an isotropic unified plasticity theory to represent the behavior of each of the component materials. A recent combined numerical and experimental investigation on the fatigue life of a metal matrix composite is reported by Foulk et al. (1998). Another investigation by Gao and Xiang (1999) examined the stress distribution in the vicinity of cracks in a cross-ply metal matrix composite.

An alternative approach to model anisotropic materials by unified elastic-viscoplastic constitutive equations is to generalize the isotropic formulation. A possible procedure on the continuum level is to redefine the stress invariant in the basic kinetic equation to apply to anisotropic media and to suitably readjust the hardening parameters. Such an exercise was performed by Robinson and Miti-Kavuma who introduced an effective stress defined in terms of invariants which reflected local transverse isotropy. In this generalized model, the

strong initial anisotropy is a dominant feature. Numerical examples indicate good agreement with test results for a metal matrix composite.

Other generalized continuum models have been developed by various investigators to specifically treat polymer matrix composites. An exercise to generalize the B-P equations for that purpose was performed by Yoon and Sun (1991). This seems to be a subject of continuing active research.

7. Summary - Status of the B-P Constitutive Theory

At this stage, the B-P constitutive theory is well developed and provides a set of equations that adequately represents the main features of rate dependent inelastic behavior of metals and alloys. Relatively few material parameters appear in the equations and these could generally be related to specific response characteristics which indicates a satisfactory physical basis of the governing equations. As a consequence, the parameters have physical interpretations and their values can be obtained from a limited band of conventional test data such as stress-strain curves at constant strain rates. Techniques for parameter identification from such test data have been devised. The equations have been incorporated into finite element and finite difference computer programs with applications over a very wide range of strain rates and temperatures. They appear to be suitable for characterizing components of composite materials and can serve as a basis for failure criteria of ductile metals.

A response condition that has not been fully examined by the B-P theory is cyclic loading with repeated load reversals and the associated matter of ratchetting. Some work has been done on cyclic loading of a high temperature alloy and on annealed copper for which the basic B-P equations appear to be adequate. However, certain materials and particularly stainless steels indicate more complex behavior which requires modification of the hardening evolution equations. These conditions have received attention from a number of investigators using unified theories with the "back stress" approach; particularly by Chaboche and colleagues in France and Ohno and colleagues in Japan. It seems that comparable modifications of the B-P equations could be readily performed. As discussed in this article, both the "directional hardening" and "back stress" variables are admissible macroscopic representations of potentially reversible hardening effects.

References

- Aboudi, J. (1991), *Mechanics of composite materials*, Elsevier Pub. Amsterdam.
- Allen, D.H. and Harris, C.E. (1990), Nonlinear constitutive behavior of metals, NASA Technical Memorandum 102727, NASA Langley Research Center, Hampton VA 23665.
- Bass, J.M. and Oden, J.T. (1988), Numerical solution of the evolution equations of damage and rate-dependent plasticity, *Int J Engng Sci* **26**(7) 713-740.
- Bell, J.F. (1973), The experimental foundations of solid mechanics, VIa/1, *Encyclopedia of Physics*, S Flugge (ed), Springer-Verlag, Berlin.
- Bodner, S.R. (1968), Constitutive equations for dynamic material behavior, *Mechanical Behavior of Materials under Dynamic Loads*, US Lindholm (ed), Springer-Verlag, New York 176-190.
- Bodner, S.R. and Partom, Y. (1972a), Dynamic inelastic properties of materials, Part II - Representation of time-dependent properties of metals, *Proc 8th Congress Int Council of Aeronaut Sci (ICAS)*, Amsterdam.
- Bodner, S.R. and Partom, Y. (1972b), A large deformation elastic-viscoplastic analysis of a thick-walled spherical shell, *ASME J Appl Mech* **39** 741-757.
- Bodner, S.R. and Partom, Y. (1975), Constitutive equations for elastic-viscoplastic strain-hardening materials, *ASME J Appl Mech* **42** 385-389.
- Bodner, S.R. (1979), Representation of time dependent mechanical behavior of René 95 by constitutive equations, Technical Report AFML-TR-79-4116, Air Force Materials Laboratory, Wright-Patterson Air Force Base, Ohio.
- Bodner, S.R. Partom, I. and Partom, Y. (1979), Uniaxial cyclic loading of elastic-viscoplastic materials, *ASME J Appl Mech* **46** 805-810.
- Bodner, S.R. and Aboudi, J. (1983), Stress wave propagation in rods of elastic-viscoplastic material, *Int J Solids Structs* **19**(4) 305-314.
- Bodner, S.R. and Chan, K.S. (1986), Modeling of continuum damage for application in elastic-viscoplastic constitutive equations, *Engng Fract Mechanics* **25**(5/6) 705-712.
- Bodner, S.R. (1987), Review of a unified elastic-viscoplastic theory, *Unified Constitutive Equations for Creep and Plasticity*, AK Miller (ed), Elsevier Applied Science, London 273-301.

- Bodner, S.R. (1991), Further development of a viscoplastic constitutive model for high temperature applications, *High Temperature Constitutive Modeling - Theory and Application*, AD Freed and KP Walker (eds) Amer. Soc. Mech. Engin. New York 175-184.
- Bodner, S.R. Naveh, M. and Merzer, A.M. (1991), Deformation and buckling of axisymmetric viscoplastic shells under thermomechanical loading, *Int J Solids Struct* **27**(15) 1915-1924.
- Bodner, S.R. and Rubin, M.B. (1994), Modeling of hardening at very high strain rates, *J Appl Phys* **76**(5) 2742-2747.
- Bodner, S.R. and Lindenfeld, A. (1995), Constitutive modelling of the stored energy of cold work under cyclic loading, *Eur J Mech A/Solids* **14**(3) 333-348.
- Bodner, S.R. and Rajendran, A.M. (1996), On the strain rate and temperature dependence of hardening of copper, *Proc. of the Conf. of the Amer. Physical Society, Topical Group on Shock Compression of Condensed Matter*, Seattle, Washington (1995), AIP Press, 499-502.
- Brace, F.W. Paulding, B.W. Jr. and Scholz, C. (1966), Dilatancy in the fracture of crystalline rocks, *J Geophysical Research* **71**(16) 3939-3953.
- Bushnell, D. (1985), *Computerized buckling analysis of shells*, Martinus Nijhoff, Pub., Dordrecht.
- Carlson, R.L. (1956), Time-dependent tangent modulus applied to column creep buckling, *ASME J Appl Mech* **13** 390-394.
- Chaboche, J.L. (1993a), Cyclic viscoplastic constitutive equations, Part I: A thermodynamically consistent formulation, *ASME J Appl Mech* **60** 813-821.
- Chaboche, J.L. (1993b), Cyclic viscoplastic constitutive equations, Part II: stored energy - comparison between models and experiments, *ASME J Appl Mech* **60** 822-828.
- Chan, K.S. Lindholm, U.S. Bodner, S.R. and Walker, K.P. (1984) A survey of unified constitutive theories, *Nonlinear Constitutive Relations for High Temperature Applications*. NASA, CP-2369 1-23.
- Chan, K.S. (1988), The constitutive representation of high-temperature creep damage, *Int J Plasticity* **4** 355-370.

- Chan, K.S. Bodner, S.R. and Lindholm, U.S. (1988), Phenomenological modeling of hardening and thermal recovery in metals, *ASME J Engng Materials Techn* **110** 1-8.
- Chan, K.S. Lindholm, U.S. Bodner, S.R. and Walker, K.P. (1989), High temperature inelastic deformation under uniaxial loading: theory and experiment, *ASME J Engng Materials Techn* **111** 345-353.
- Chan, K.S. Lindholm, U.S. Bodner, S.R. and Nagy, A. (1990a), High temperature inelastic deformation of the B1900+Hf alloy under multiaxial loading: theory and experiment, *ASME J Engng Materials Techn* **112** 7-14.
- Chan, K.S. and Lindholm, U.S. (1990b), Inelastic deformation under nonisothermal loading, *ASME J Engng Materials Techn* **112** 15-25.
- Chan, K.S. Bodner, S.R. Fossum, A.F. and Munson, D.E. (1992), A constitutive model for inelastic flow and damage evolution in solids under triaxial compression, *Mech Mat* **14** 1-14.
- Chan, K.S. Bodner, S.R. and Munson, D.E. (1998), Recovery and healing of damage in WIPP salt, *Inter J Damage Mechanics* **7** 143-166.
- Chan, K.S. Munson, D.E. and Bodner, S.R. (1999), Creep deformation and fracture in rock salt, *Fracture of Rock*, MH Aliabadi (ed), Computation Mechanics Pub., WIT Press, Southampton UK.
- Cook, W.H. Rajendran, A.M. and Grove, D.J. (1992), An efficient numerical implementation of the Bodner-Partom model in the EPIC-2 code, *Eng Fract Mechs* **41**(5) 607-623.
- Dexter, R.J. Hudak, S.J. Jr. Reed, K.W. Polch, E.Z. and Kanninen, M.F. (1987), Dynamic-viscoplastic analysis and small-specimen experimental methods for the study of fracture in A533B steel, *Numer Methods in Fract Mechs. Proc 4th Int Conf* San Antonio, Texas, AR Luxmoore, DRI Owen, YPS Rajapakse, MF Kanninen (eds) 173-190.
- Dexter, R.J. and Chan, K.S. (1990), Viscoplastic characterization of A533B steel at high strain rates, *ASME J Pressure Vessel Techn* **112** 218-224.
- Dexter, R.J. Chan, K.S. and Coutts, W.H. (1991), Elastic-viscoplastic finite element analysis of a forging die, *Int J Mech Sci* **33** 659-674.

- Dombrovsky, L.A. (1992), Incremental constitutive equations for Miller and Bodner-Partom viscoplastic models, *Computers & Structures* **44** 1065-1072.
- Doong, S-H. Socie, D.F. and Robertson, I.M. (1990), Dislocation substructures and nonproportional hardening, *ASME J Engng Materials Techn* **112** 456-464.
- Eftis, J. Abdel-Kader, M.S. Jones, D.L. (1989), Comparisons between the modified Chaboche and Bodner-Partom viscoplastic constitutive theories at high temperature, *Inter J Plasticity* **5** 1-27.
- Estrin, Y. and Mecking, H. (1986), An extension of the Bodner-Partom model of plastic deformation, *Int J Plasticity* **2** 73-85.
- Follansbee, P.S. and Kocks, U.F. (1988), A constitutive description of the deformation of copper based on the use of mechanical threshold stress as an internal state variable, *Acta Metall* **36**(1) 81-93.
- Fossum, A.F. (1998), Rate data and material model parameter estimation, *ASME J Engng Materials Tech* **120** 7-12.
- Foulk, J.W. III, Allen, D.H. and Helms, K.L.E. (1998), A model for predicting the damage and enviromental degradation life of SCS-6/Timetal[®] 21S[0]₄ metal matrix composite, *Mechanics of Materials* **29** 53-68.
- Freed, A.D. and Walker, K.P. (eds) (1991), *High Temperature Constitutive Modeling - Theory and Application*, Amer Soc Mech Engin, New York.
- Gao, Z.J. and Xiang, X.Y. (1999) A variational approach to analyzing laminates with cracks and viscoplasticity - the model and its validation. *J Composite Materials* **33** 443-479.
- Gerard, G. (1956), A creep buckling hypothesis. *J Aero Sci* **23** 879-.
- Gilat, A. and Tsai, J. (1990), Application of Bodner viscoplastic theory to pressure-shear plate impact experiment. *ASME J Engng Materials Techn* **112** 52-55.
- Gray, G.T. III Chen, S.R. Wright, W. and Lopez, M.F. (1994), LA-12669-MS, Los Alamos National Laboratory Report.

- Halford, G.R. (1966), *Stored energy of cold work changes induced by cyclic deformation*, Ph.D. thesis, Dept. Theoretical and Applied Mechanics, U. Illinois Urbana, Illinois. Also, (2000) www.eJournal-of-Mechanics.org
- Hayhurst, D.R. (1972), Creep rupture under multi-axial state of stress, *J Mech Phys Solids* **20** 381-390.
- Hill, R. (1950), *The mathematical theory of plasticity*, Clarendon Press, Oxford.
- Hill, R. (1958), A general theory of uniqueness and stability in elastic-plastic solids, *J Mech Phys Solids* **6** 236-249.
- Hill, R. (1994), Classical plasticity: a retrospective view and a new proposal, *J Mech Phys Solids* **42** 1803-1816.
- Holian, B.L. and Lomdahl, P.S. (1998), Plasticity induced by shock waves in nonequilibrium molecular-dynamics simulations, *Science* **280** 2085-2088.
- Huang, S. and Kahn, A.S. (1992), Modeling the mechanical behavior of 1100-0 aluminum at different strain rates by the Bodner-Partom model, *Int J Plasticity* **8** 501-517.
- James, G.H. Imbrie, P.K. Hill, P.S. Allen, D.H. and Haisler, W.E. (1987), An experimental comparison of current viscoplastic models at elevated temperature, *ASME J Engng Materials Techn* **109** 130-139.
- Jinghong, F. and Xianghe, P. (1991), A physically based constitutive description for nonproportional cyclic plasticity, *ASME J Engng Materials Techn* **113** 254-262.
- Kachanov, L.M. (1958), On the time to failure under creep conditions, *Izv Akad Nauk SSSR* **8** 26-31.
- Khen, R. and Rubin, M.B. (1992), Analytical modelling of second order effects in large deformation plasticity, *Int J Solid Structures* **29** 2235-2258.
- Klepaczko, J.R. and Cheim, C.Y. (1986), On rate sensitivity of fcc metals, instantaneous rate sensitivity and rate sensitivity of strain hardening, *J Mech Phys Solids* **34** 29-54.
- Kolkailah, F.A. and McPhate, A.J. (1990), Bodner-Partom constitutive model and nonlinear finite element analysis, *ASME J Engng Materials Tech* **112** 287-291.

- Kollman, F.G. and Sansour, C. (1997), Viscoplastic shells, theory and numerical analysis, *Archives of Mechanics* **49** 477-511.
- Krajcinovic, D. (1996), *Damage mechanics*. Elsevier Pub. Amsterdam.
- Krausz, A.S. (ed) (1996), *Constitutive Laws of Plastic Deformation*. Academic Press, New York.
- Lemaitre, J. (1992), *A course on damage mechanics*. Springer-Verlag, Berlin.
- Li, K. and Sharpe, W.N. Jr. (1996), Viscoplastic behavior of a notch root at 650°C: ISDG measurement and finite element modelling, *ASME J Engng Materials Tech* **118** 88-93.
- Lipkin, J. Campbell, J.D. and Swearngen, J.C. (1978), The effects of strain-rate variations of the flow stress of OFHC copper, *J Mech Phys Solids* **26** 251-268.
- Mahnken, R. and Stein, E. (1996), Parameter identification for viscoplastic models based on analytical derivatives of a least-squares functional and stability investigations, *Int J Plasticity* **12**(4) 451-479.
- Massin, P. Triantafyllidis, N. and Leroy, Y.M. (1999), On the stability of strain-rate dependent solids. I - structural examples, *J Mech Phys of Solids* **47** 1737-1779.
- Merzer, A. and Bodner, S.R. (1979), Analytical formulation of a rate and temperature dependent stress-strain relation, *ASME J Engrg Materials Techn* **101** 254-257.
- Merzer, A.M. (1982), Steady and transient creep behavior based on unified constitutive equations, *ASME J Engng Materials Tech* **104** 18-25.
- Mikkelsen, L.P. (1993), On the analysis of viscoplastic buckling, *Int J Solids Structs* **30**(11) 1461-1472.
- Miller, A.K. (ed) (1987), *Unified Constitutive Equations for Plastic Deformation and Creep of Engineering Alloys*, Elsevier Applied Science, New York.
- Miller, A.K. (1987), The MATMOD equations, *Unified Constitutive Equations for Creep and Plasticity*, AK Miller (ed), Elsevier Applied Science, London 139-219.
- Mizuno, M. Mima, Y. Abdel-Karim M and Ohno, O (2000), Uniaxial ratchetting of 316FR steel at room temperature - Part I: Experiments, *ASME J Eng Mats and Techn* **122**.

- Moreno, V. and Jordan, E.H. (1986), Prediction of material thermomechanical response with a unified viscoplastic constitutive model, *Int J Plasticity* **2** 223-245.
- Nabarro, F.R. and Filmer, H. (1993), *Physics of creep and creep resistant alloys*, Taylor and Francis, Pub., Philadelphia.
- Neu, R.W. and Bodner, S.R. (1995), Determination of the material constants of Timetal 21S for a constitutive model, Report on Contract F33615-94-C-5804, Wright Laboratory, Materials Directorate, Wright-Patterson AFB, Ohio.
- Newman, M. Zaphir, Z. and Bodner, S.R. (1976), Finite element analysis for time-dependent inelastic material behavior, *J Computers and Structures* **6** 157-162.
- Nicholas, T. Rajendran, A.M. and Grove, D.J. (1987), Analytical modeling of precursor decay in strain-rate dependent materials, *Int J Solids Structs* **23** 1601-1614.
- Nicholas, T. and Rajendran, A.M. (1990), Material characterization at high strain rates, *High Velocity Impact Dynamics*, JA Zukas (ed), John Wiley & Sons, New York, 127-296.
- Nicholas, T. Kroupa, J.L. and Neu, R.W. (1993), Analysis of a [0°/90°] metal matrix composite under thermomechanical fatigue loading, *Composites Engineering* **3** 675-689.
- Obrecht, H. (1977), Creep buckling and postbuckling of circular cylindrical shells under axial compression, *Int J Solid Structures*, **13**, 337-355.
- Ohno, N. (1990), Recent topics on constitutive modeling of cyclic plasticity and viscoplasticity, *ASME Appl Mech Rev* **43**(11) 283-295.
- Ohno, N. and Wang, J.D. (1993), Kinematic hardening rules with critical state of dynamic recovery, Part I - Formulation and basic features for ratchetting behavior, Part II - Application to experiments of ratchetting behavior, *Int J Plasticity* **9**(3) 375-403.
- Ohno, O. and Abdel-Karim, M. (2000), Uniaxial ratchetting of 316FR steel at room temperature - Part II: Constitutive modeling and simulation, *ASME J Eng Mats and Techn* **122**.
- Orowan, E. (1947),
J West of Scotland Iron and Steel Institute **54** 45.
- Orowan, E. (1959), Causes and effects of internal stresses, *Internal Stresses and Fatigue in Metals*, GM Rassweiler, WL Grube (eds), Elsevier Publishers, Amsterdam 59-80.

- Paley, M. and Aboudi, J. (1991a) Viscoplastic bifurcation buckling of plates, *AIAA J* **29** 627-632.
- Paley, M. and Aboudi, J. (1991b) Plastic buckling of metal matrix laminated plates, *Int J Solids Structures* **28**(9) 1139-1154.
- Pandey, A.K. Dechaumphai, P. and Thornton, E.A. (1991), Finite element thermoviscoplastic analysis of aerospace structures, *Thermal Structures and Materials for High Speed Flight*, EA Thornton (ed), *AIAA* **140**.
- Rabotnov, G.N. and Shesterikov, A. (1957), Creep stability of columns and plates, *J Mech Phys Solids*, **6** 27-34.
- Rabotnov, G.N. (1968), Creep rupture, *Proc. 12th IUTAM Cong Appl Mech*. Stanford, Springer, Berlin.
- Rajendran, A.M. Bless, S.J. and Dawicke D.S. (1986), Evaluation of Bodner-Partom model parameters at high strain rates, *ASME J Engng Materials Techn* **108** 75-80.
- Rajendran, A.M. and Grove, D.J. (1987), Bodner-Partom viscoplastic model in STEALTH finite difference code, AFWAL-TR-86-4098, Materials Laboratory, WPAFB, OH, 45433.
- Rajendran, A.M. Dietenberger, M.A. and Grove, D.J. (1989), A void-growth based failure model to describe spallation, *J Appl Phys* **65** 1521-1527.
- Robinson, D.N. and Miti-Kavuma, M. (1989), An anisotropic extension of Bodner's model of viscoplasticity: application to SiC/Ti.
- Rowley, M.A. and Thornton, E.A. (1996), Constitutive modeling of the visco-plastic response of Hastelloy-X and aluminum alloy 8009, *ASME J Engng Materials Tech* **118** 19-27.
- Rubin, M.B. (1986), An elastic-viscoplastic model for large deformation, *Int J Engng Sci* **24**(7) 1083-1095.
- Rubin, M.B. (1987), An elastic-viscoplastic model exhibiting continuity of solid and fluid states, *Int J Engng Sci* **25**(9) 1175-1191.

- Rubin, M.B. (1989), A time integration procedure for large plastic deformation in elastic-viscoplastic metals, *J Math and Physics (ZAMP)* **40** 846-871.
- Rubin, M.B. and Bodner, S.R. (1995), An incremental elastic-viscoplastic theory indicating a reduced modulus for non-proportional buckling, *Int J Solids Struct* **32** 2967-2987.
- Sansour, C. and Kollman, F.G. (1997), On theory and numerics of large viscoplastic deformation, *Computer Methods in Applied Mechs and Engng* **146** 351-369.
- Sansour, C. and Kollman, F.G. (1998), Large viscoplastic deformations in shells; theory and finite element formulation, *Comput Mech* **21**(6) 512-525.
- Senchenkov, I.K. and Tabieva, G.A. (1996), Determination of the parameters of the Bodner-Partom model for thermoviscoplastic deformation of materials, *Int Appl Mechs* **32**(2) 132-139. (Translated from *Prikladnaya Mekhanika* **32**(2) 64-72 Feb. 1996.)
- Senchenkov, I.K. and Zhuk, Y.A. (1997) Thermoviscoplastic deformation of materials, *Int Appl Mechs* **33**(2) 122-128.
- Senseney, P.E. and Fossum, A.F. (1995), On testing requirements for viscoplastic constitutive parameter estimation, *ASME J Engin Mat Tech* **117** 151-156.
- Simitses, I. Song, Y. and Sheinman, I. (1991), Elastoviscoplastic snap-through behavior of shallow arches subjected to thermomechanical loads, *Finite Elements in Analysis and Design* **10** 151-163.
- Skipor, A.F. Harren, S.V. and Botsis, J. (1996), On the constitutive response of 63/37 Sn/P_b eutectic solder, *ASME J Engng Materials Tech* **118** 1-11.
- Sleeswyk, A.W. Kassner, M.E. and Kemerink, G.J. (1986) The effect of partial reversibility of dislocation motion, *Large Deformation of Solids*, U Gittus, J Zarka, S Nemat-Nasser (eds), Elsevier Applied Science, London, 81-98.
- Smail, J. and Palazotto, A.N. (1984), The viscoplastic crack growth behavior of a compact tension specimen using the Bodner-Partom flow law, *Engng Fract Mechs* **19**(1) 137-158.
- Stouffer, D.C. (1981), A constitutive representation for IN-100 AFWAL-TR-81-4039, Wright-Patterson AFB, OH.

Sung, J.C. and Achenbach, J.D. (1987), Temperature at a propagating crack tip in a viscoplastic material, *J Thermal Stresses* **10** 243-262.

Tanaka, T.G. and Miller, A.K. (1988), Development of a method for integrating time-dependent constitutive equations with large, small or negative strain rate sensitivity, *Int J Numer Methods Eng* **26** 2457-2485.

Tong, W. Clifton, R.J. and Huang, S. (1992), Pressure-shear impact investigation of strain rate history effects in oxygen - free high-conductivity copper, *J Mech Phys Solids* **40** 1251-1294.

Tvergaard, V. (1989), Plasticity and creep at finite strains, *Proc. 17th Congress of Theoretical and Applied Mechanics*, P Germain, M Piau and D Cailline (eds), Elsevier Science Pub. Amsterdam 349-368.

Wyatt, O.H. (1953), Transient creep in pure metals, *Proc. Phys Soc* **66B** 459-480.

Yoon, K.J. and Sun, C.T. (1991), Characterization of elastic-viscoplastic properties of an AS4/PEEK thermoplastic composite, *J Composite Mat* **25** 1277-1298.

Zaphir, Z. and Bodner, S.R. (1979) Implementation of elastic-viscoplastic constitutive equations into 'NONSAP' with applications to fracture mechanics, *Proceedings, ADINA Conference*, KJ Bathe (ed), MIT Report 82448-9.

Zeng, H. and Sharpe, W.N. (1997), Biaxial creep strains at notch roots - measurement and modeling, *ASME J Engng Materials Techn* **119** 46-50.

Zhu, Y.Y. and Cescotto, S. (1991), The finite element prediction of ductile fracture initiation in dynamic metal-forming processes, *J Physique III*, **1**.

Zukas, J.A. (1994), Numerical simulation of high rate behavior, *Shock and Impact on Structures*, CA Brebbia, V Sanchez-Galvez (eds), Computational Mechanics Pub, Southampton UK 1-26.

Appendix A

Computer Program for Uniaxial Stress and Isotropic and Directional Hardening (by M.B. Rubin)

The following Program was executed using

MATLAB Version 5.2.0.3084

The Math Works, Inc.

```
function Visco
```

```
% Visco is the main program that calculates the response of an  
% elastic viscoplastic metal for uniaxial stress
```

```
global mat sigt dtt Z jp1 stres
```

```
%-----
```

```
% Specify the material constants
```

```
mat = zeros(1,8);
```

```
E      = 200.0;           % Young's modulus (GPa)  
D0     = 1.0e+8;          % Controls maximum plastic strain rate (1/s)  
n      = 1.0;            % Controls rate sensitivity  
Z0     = 10.0;           % Initial value of isotropic hardening ZI (GPa)  
Z1     = 15.0;           % Maximum value of ZI (GPa)  
m1     = 0.05e+3;         % Controls rate of isotropic hardening (1/GPa)  
Z3     = 5.0;            % Maximum value of directional hardening ZD (GPa)  
m2     = 0.15e+3;         % Controls rate of directional hardening (1/GPa)
```

```
mat(1) = E;  
mat(2) = D0;  
mat(3) = n;  
mat(4) = Z0;  
mat(5) = Z1;  
mat(6) = m1;  
mat(7) = Z3;  
mat(8) = m2;
```

```
%-----
```

```
% Specify the specify number of loading cycles
```

```
nload      = 1;          % Number of loading cycles
```

```
% Specify cycle 1
```

```
nstep(1)   = 400;        % Number of steps in the cycle  
e11f(1)    = 5.0e-2;     % Final value of the total strain for the cycle  
rate(1)     = 1.0e-3;     % Magnitude of the total strain rate for the cycle (1/s)
```

```

                                %      If rate = 0 then it is assumed that relaxation
occurs
dtrel(1)      = 0.0;           %      Relaxation time for the cycle. If rate is positive then
                                the magnitude of dtrel is ignored

%      Specify cycle 2
nstep(2)      = 400;
e11f(2)       = -2.5e-2;
rate(2)       = 1.0e-3;
dtrel(2)      = 0.0e+0;

%      Specify cycle 3
nstep(3)      = 400;
e11f(3)       = 2.5e-2;
rate(3)       = 1.0e-3;
dtrel(3)      = 0.0;

%      Specify cycle 4
nstep(4)      = 400;
e11f(4)       = -2.5e-2;
rate(4)       = 1.0e-3;
dtrel(4)      = 0.0e+0;

%-----
%      Calculate the total number of steps
ntotal = 0;
for i=1:nload;
    ntotal = ntotal + nstep(i);
end

%-----
%      Initialize the stres array
%      stres(:,1) = time (s);
%      stres(:,2) = e11 = total strain
%      stres(:,3) = ep11 = plastic strain;
%      stres(:,4) = ZI = isotropic hardening (GPa);
%      stres(:,5) = bet11 = directional hardening parameter (GPa);
%      stres(:,6) = ZD = directional hardening (GPa);
%      stres(:,7) = sig11 = axial stress (GPa);
%      stres(:,8) = dWp = rate of plastic work (GPa);
%      stres(:,9) = value of the function f;
stres = zeros(ntotal+1,9);
stres(1,4) = Z0;

%-----

```



```

%      Calculate the time increments for each step
dt = zeros(nload);
rate(1) = sign(e11f(1)) *rate(1);
dt(1) = e11f(1)/rate(1)/nstep(1);
for i=2:nload
    if rate(i)>0.0
        de11 = e11f(i)-e11f(i-1);
        rate(i) = sign(de11) *rate(i);
        dt(i) = de11/rate(i)/nstep(i);
    else
        dt(i) = dtrel(i)/nstep(i);
    end
end

%-----
%      Calculate the response
istep = 0;
for i=1:nload;
    for jj=1:nstep(i);
        %      Calculate time
        dtt = dt(i);
        j = istep + jj;
        jp1 = j + 1;
        stres(jp1,1) = stres(j,1) + dtt;
        %      Calculate total strain
        stres(jp1,2) = stres(j,2) + dtt*rate(i);
        %      Calculate elastic trial value of stress
        sigt = E*(stres(j+1,2) - stres(j,3));
        %      Calculate the scale factor lamda
        Z = stres(j,4) + stres(j,6);          %      Use old value of hardening Z
        lamda = 1.0;                          %      Initial guess for lamda
        lamda = fzero('fun',lamda);
        %      Calculate stress
        stres(jp1,7) = lamda*sigt;
        %      Calculate plastic strain
        stres(jp1,3) = stres(jp1,2) - stres(jp1,7)/E;
        %      Calculate increment of plastic work
        dtWp = lamda*(1.0-lamda)*sigt^2/E;
        %      Calculate rate of plastic work
        stres(jp1,8) = dtWp/dtt;
        %      Calculate isotropic hardening
        stres(jp1,4) = Z1 - (Z1 - stres(j,4))*exp(-m1*dtWp);
        %      Calculate directional hardening
        u11 = sign(sigt);
        stres(jp1,5) = Z3*u11 - (Z3*u11 - stres(j,5))*exp(-m2*dtWp);
        stres(jp1,6) = stres(jp1,5)*u11;
    end
end

```

```

end
istep = istep+nstep(i);
end

```

```

function f = fun(lamda)
%      The function fun determines the function
%      who's root gives the scalar value lambda

global mat sigt dtt Z jp1 stres

% Input material parameters
E      = mat(1);
D0     = mat(2);
n      = mat(3);

%      Calculate function f
sig = abs(sigt);
if     sig > 0.0
    factor = 2*dtt*D0/sqrt(3.0)*E/sig;
    f = 1.0 - lamda - factor*exp(-0.5*(Z/lamda/sig)^(2.0*n)) ;
else
    f = 0.0;
end
stres(jp1,9) = f;

```

Appendix B Nomenclature

<i>Symbol</i>	<i>Description</i>
e_{ij}	deviatoric total strain
e_{ij}^P	deviatoric plastic strain
\underline{e}	absolute value of deviatoric total strain
\dot{e}_{ij}	deviatoric total strain rate
$\underline{\dot{e}}$	absolute value of deviatoric total strain rate
\dot{e}_{ij}^P	deviatoric plastic strain rate
\dot{e}_{eff}^P	effective plastic strain rate, eq. (6a)
g,i,j,k	indices
m_1, m_2	rates of hardening (isotropic and directional)
m_{1a}, m_{1b}, m_{1c}	coefficients in expansion of m_1 , eq. (21a)
m_{2a}, m_{2b}, m_{2c}	coefficients in expansion of m_2 , eq. (21b)
n	term in kinetic equation, (7)-(10), that controls rate sensitivity and influences level of flow stress
r_1, r_2	exponents in expressions for thermal recovery of isotropic and directional hardening
s_{ij}	deviatoric stress
$\underline{\dot{s}}$	absolute value of deviatoric stress rate
u_{ij}	direction of stress, eq. (15a)
u'_{ij}	direction of deviatoric stress

v_{ij}	direction of directional hardening variable, eq. (15b)
<u>Symbol</u>	<u>Description</u>
w_{ij}	direction of plastic strain rate, eq. (19a)
y_{ij}	direction of "back stress" variable
A_1, A_2	coefficients of thermal recovery of hardening (isotropic and directional)
D_0	maximum plastic strain rate (assigned value)
D_2^p	second invariant of deviatoric plastic strain rate
E	elastic (Young's) modulus
E_T	tangent (Young's) modulus
E_T^p	plastic tangent (Young's) modulus
F	scalar function of hardening variables in expanded flow law, eq. (30).
G	elastic shear modulus
G_T	tangent shear modulus
J_2	second invariant of deviatoric stress
K	elastic bulk modulus
K_1	$= [2\ell n(2D_0 / \sqrt{3}R)]^{-(1/2n)}$, eq. (14a)
M_a	coefficient for rate dependence of hardening rate, eq. (23)
R	constant axial plastic strain rate value, in eq. (14a) for K_1
R_1	imposed (total) axial strain rate
SECW	stored energy of cold work (following G.I. Taylor)
T	current temperature
T_o, T_m	reference and melting temperatures

<u>Symbol</u>	<u>Description</u>
W_p	accumulated plastic work
\dot{W}_p	plastic work rate
Z_g	internal state variables
Z	total hardening variable ($= Z^I + Z^D$)
Z^I	isotropic hardening variable
Z_0	initial value of isotropic hardening variable
Z_1	maximum (saturated) value of isotropic hardening variable
Z_2	minimum (fully annealed) value of isotropic hardening variable
Z_3	maximum (saturated) value of directional hardening variable
Z^D	component of directional hardening variable in direction of current stress, ($= \beta_{ij} u_{ij}$), eq. (16)
α	coefficient of linear thermal expansion
α_{ij}	"back stress" or "kinematic" hardening variable
β_{ij}	directional hardening variable
γ	uniaxial engineering shear strain
$\dot{\gamma}_{ij}$	engineering shear strain rate
$\dot{\gamma}_{ij}^P$	engineering plastic shear strain rate
δ_{ij}	Kronecker delta function
$\dot{\epsilon}_{ij}$	total strain rate

$\dot{\epsilon}_{ij}^e$	elastic strain rate
<u>Symbol</u>	<u>Description</u>
$\dot{\epsilon}_{ij}^p$	plastic strain rate
$\dot{\epsilon}_{eff}^p$	effective plastic strain rate [= $\dot{\epsilon}_{eff}^p$, eq. (6a)]
ϵ^c	uniaxial creep strain
λ	coefficient in flow law
ν	elastic Poisson's ratio
σ_{ij}	stress (in general)
σ_{eff}	effective stress, eq. (6b)
σ_s	saturated (maximum) stress
σ_y	engineering yield stress
τ_{ij}	shear stress (usually used specifically for $i \neq j$)
ω	isotropic damage variable

Figures

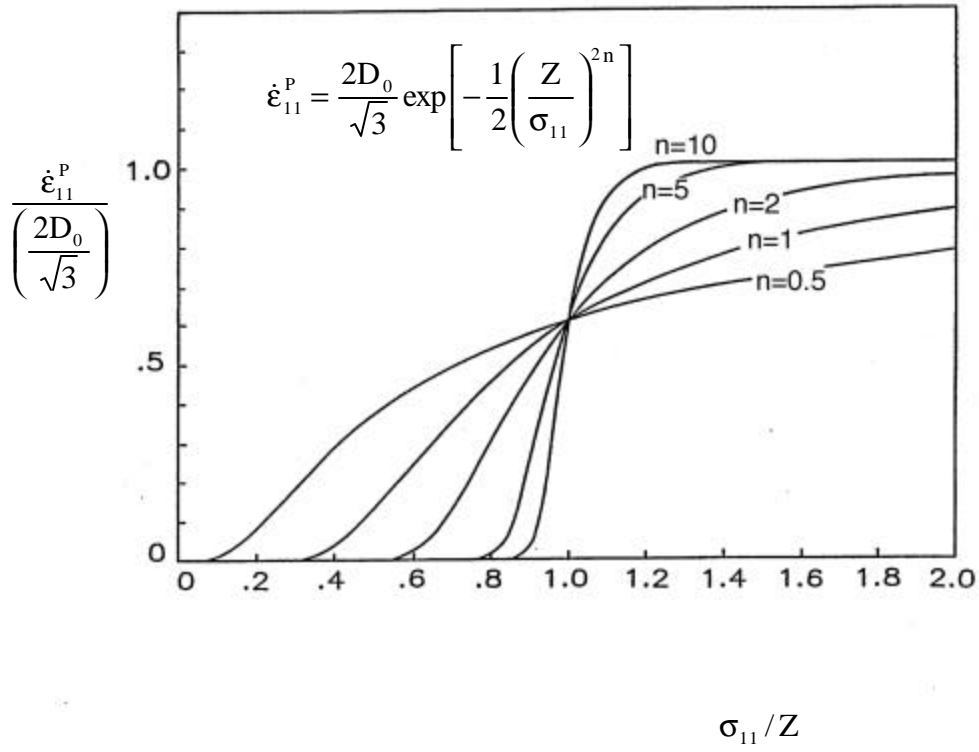


Fig. 1: Inelastic strain rates for uniaxial tension, σ_{11} , and various values of n .

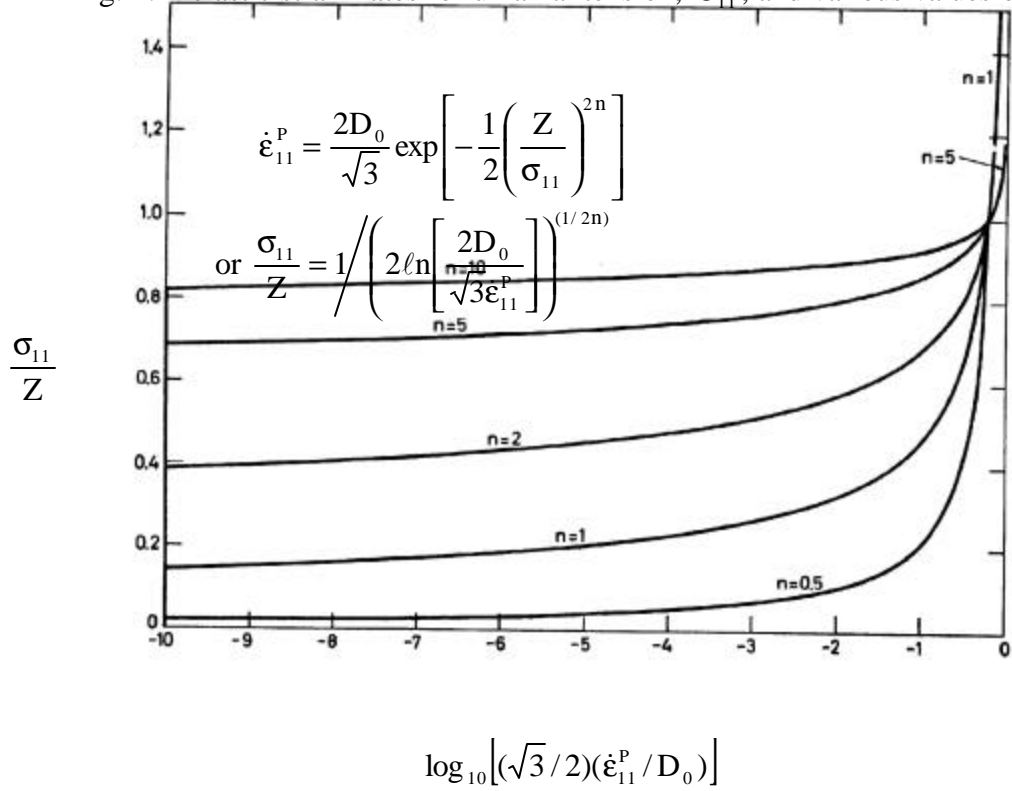
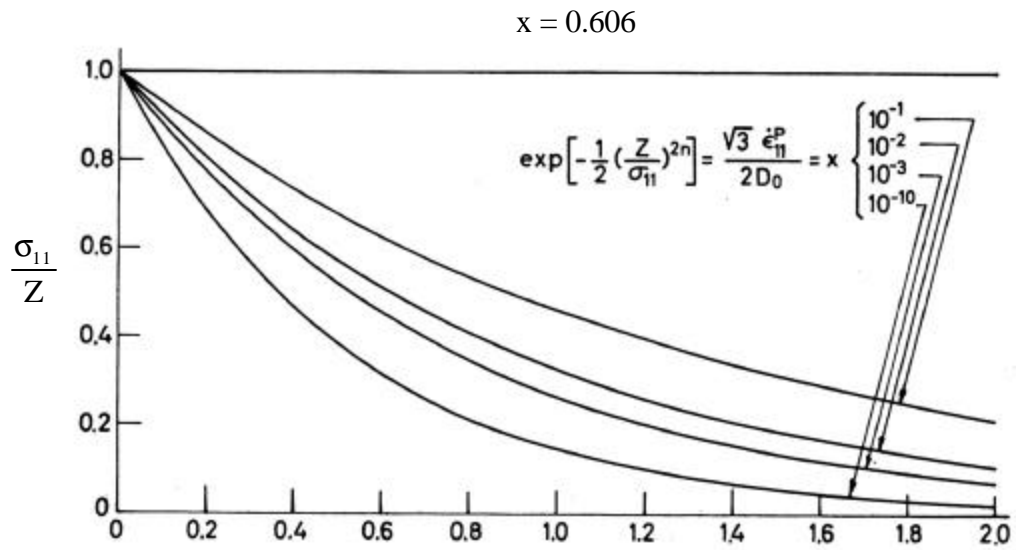


Fig. 2: Dependence of the uniaxial flow stress parameter on the strain rate parameter for various values of the strain rate sensitivity constant n .



$$(1/n) = (T/a)$$

Fig. 3: Dependence of the uniaxial flow stress parameter on the (temperature dependent) strain rate sensitivity constant n for different values of the strain rate parameter.

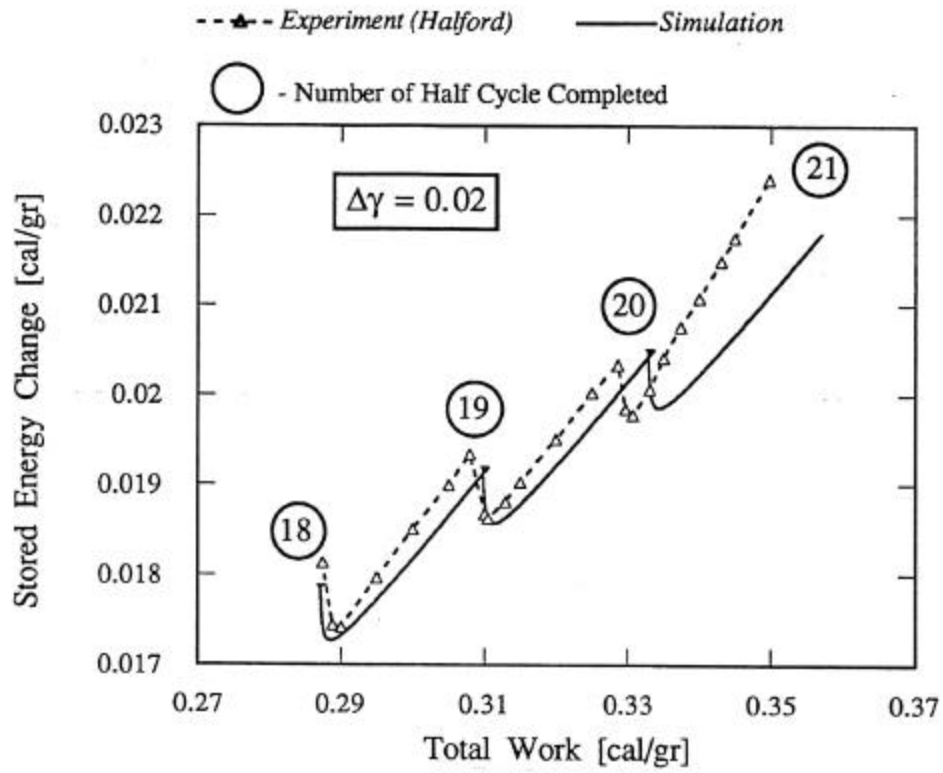


Fig. 4: Simulation by Bodner and Lindenfeld (1995) of stored energy change as a function of total work during three consecutive half cycles in comparison with Halford's experiment, Halford (1966).

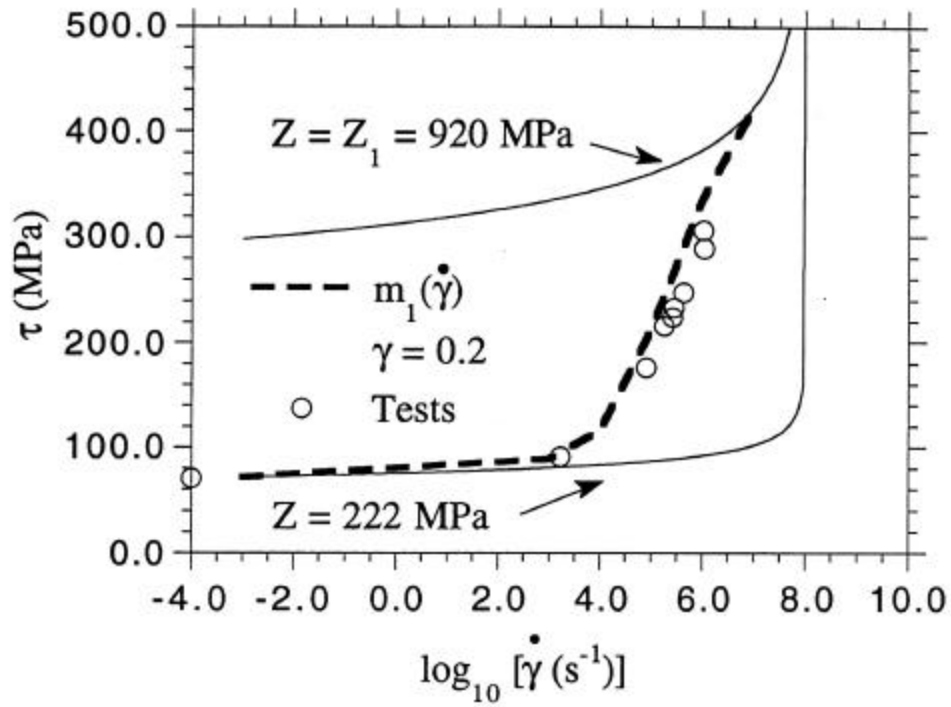


Fig. 5: Flow stress dependence of copper on logarithm of strain rate,
 (a) original B-P model for $Z = 222$ MPa (corresponding to $\gamma = 0.20$ at the lower rates), and for the stress saturation condition with $Z = Z_1 = 920$ MPa: ————
 (b) modified B-P model with strain rate dependence of the hardening rate: - - - - -
 (b) experimental points for $\gamma = 0.20$, Tong et al. (1992): ○ ○ ○
 Simulations from Bodner and Rubin (1994).

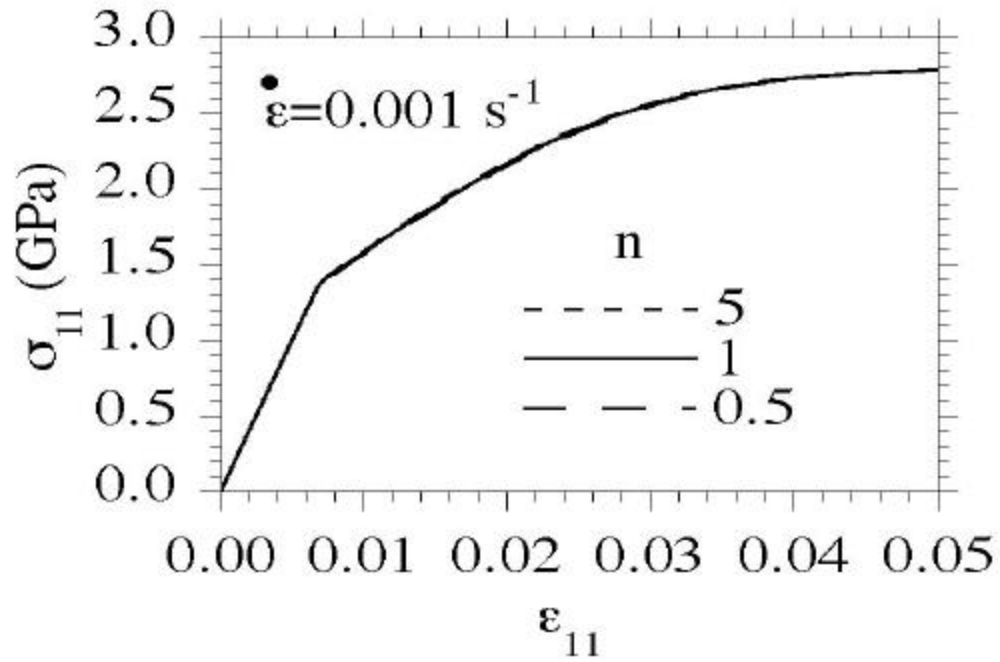


Fig. 6: Representation of identical stress-strain curves for different combinations of n and Z_0 with m_I and Z_I/Z_0 fixed.

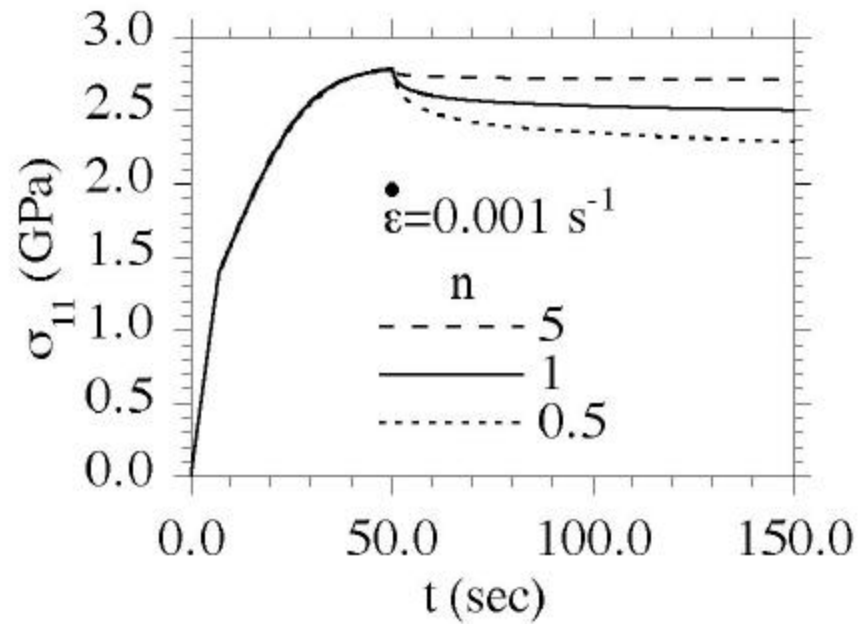


Fig. 7: Effect of rate-sensitivity parameter n on stress relaxation behavior with the same material constants used in Fig. 6.

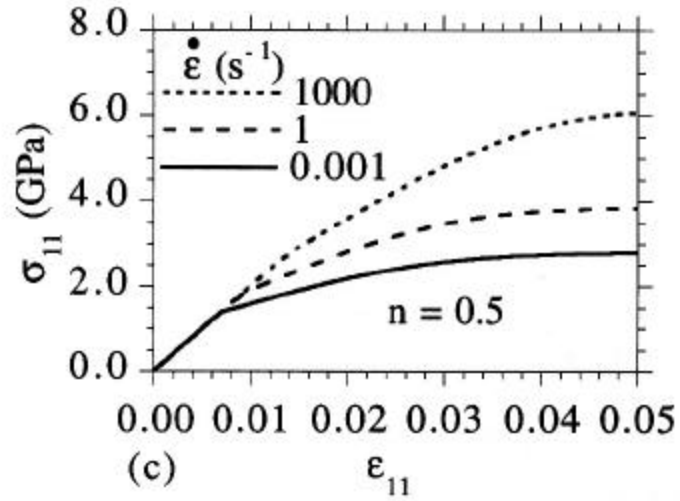
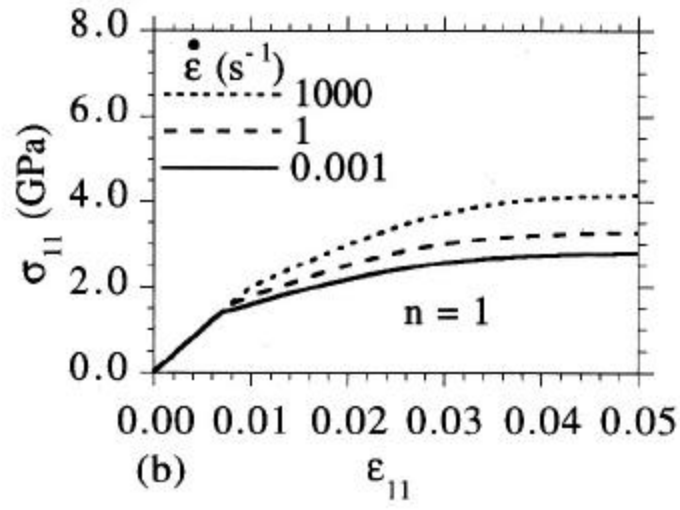
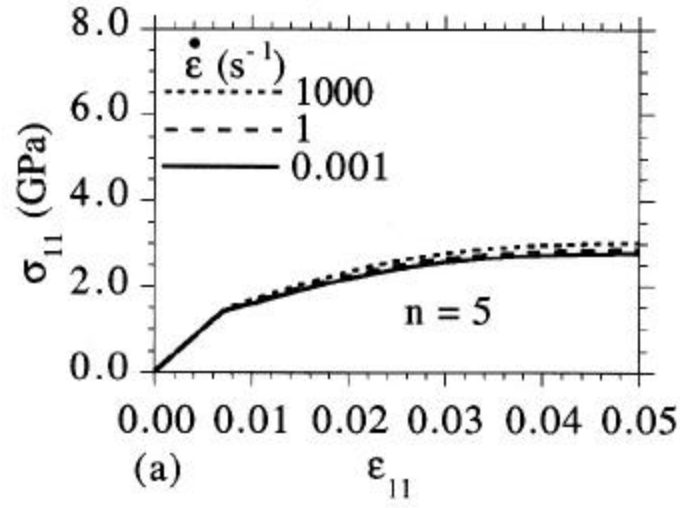


Fig. 8: Effect of rate sensitivity parameter n on stress-strain behavior at various imposed rates with the same material constants used in Figs. 6,7.

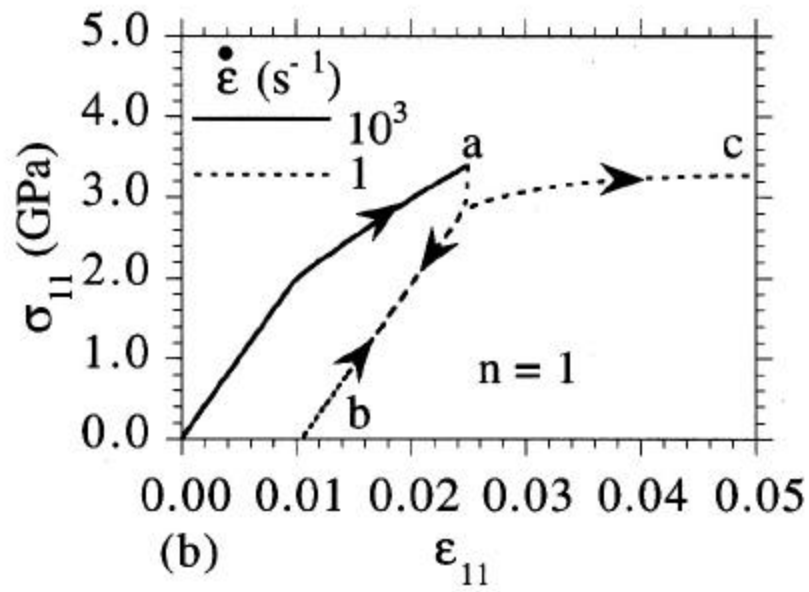
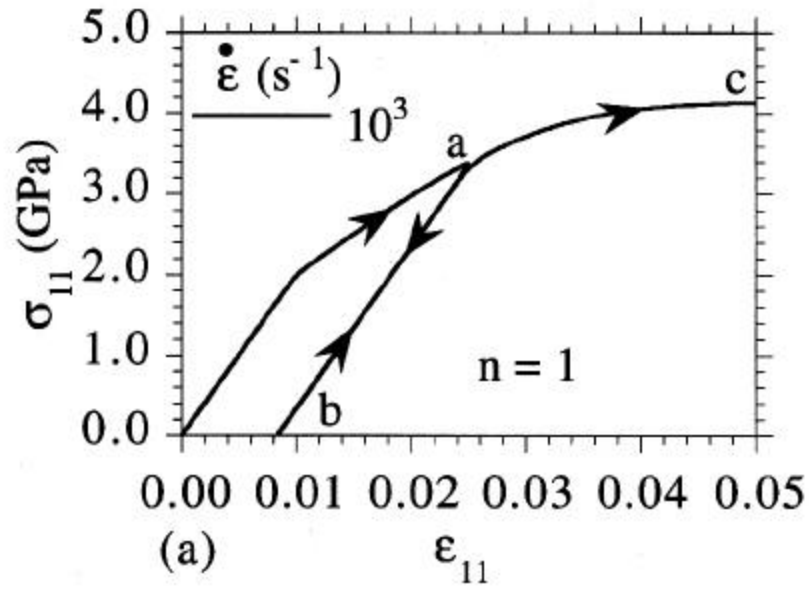


Fig. 9: Loading, unloading, and re-loading stress-strain curves for $n = 1$ and associated constants; initial loading $\dot{\epsilon} = 10^3 \text{ sec}^{-1}$;
 (a) unloading and reloading, $\dot{\epsilon} = 10^3 \text{ sec}^{-1}$;
 (b) unloading and reloading, $\dot{\epsilon} = 1 \text{ sec}^{-1}$.

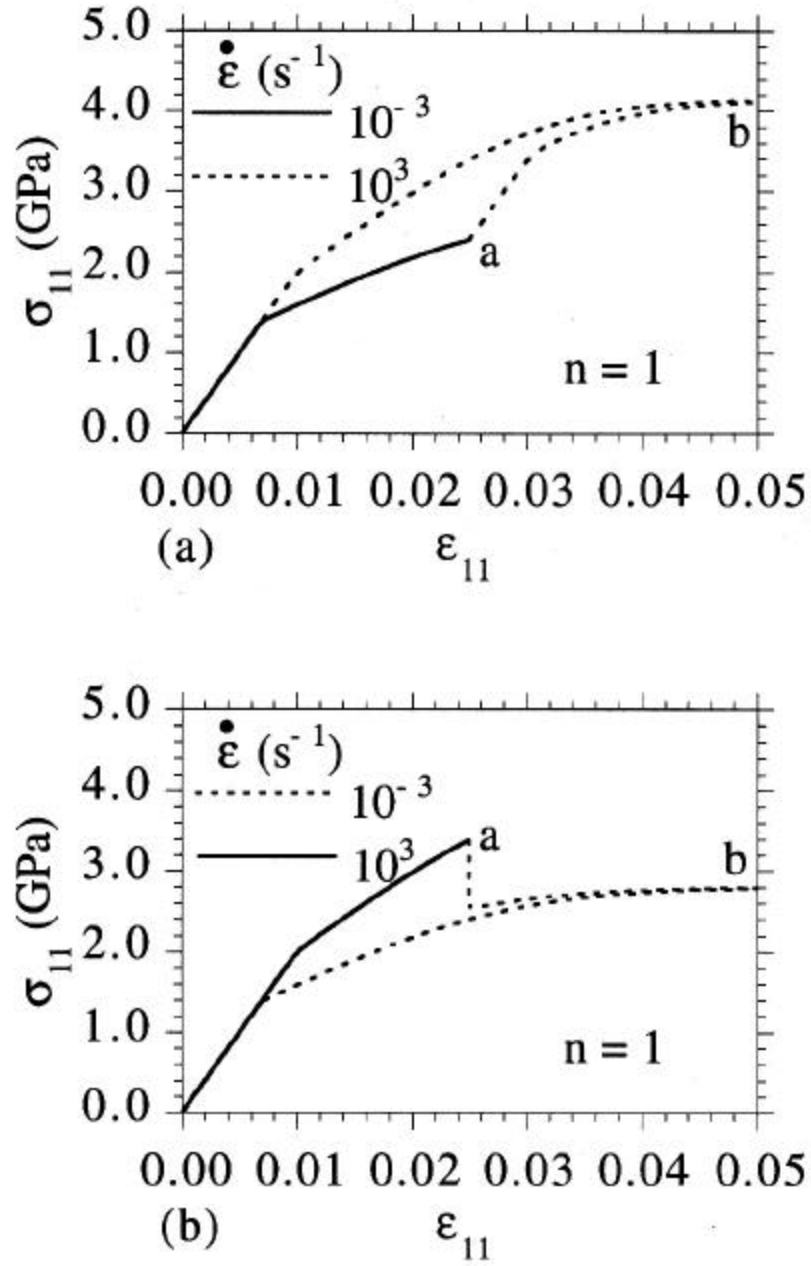


Fig. 10: Effect of changes of imposed strain rate on stress-strain response for $n = 1$ and associated constants;

(a) initial loading $\dot{\epsilon} = 10^{-3} \text{ sec}^{-1}$, secondary loading $\dot{\epsilon} = 10^3 \text{ sec}^{-1}$,

(b) initial loading $\dot{\epsilon} = 10^3 \text{ sec}^{-1}$, secondary loading $\dot{\epsilon} = 10^{-3} \text{ sec}^{-1}$.

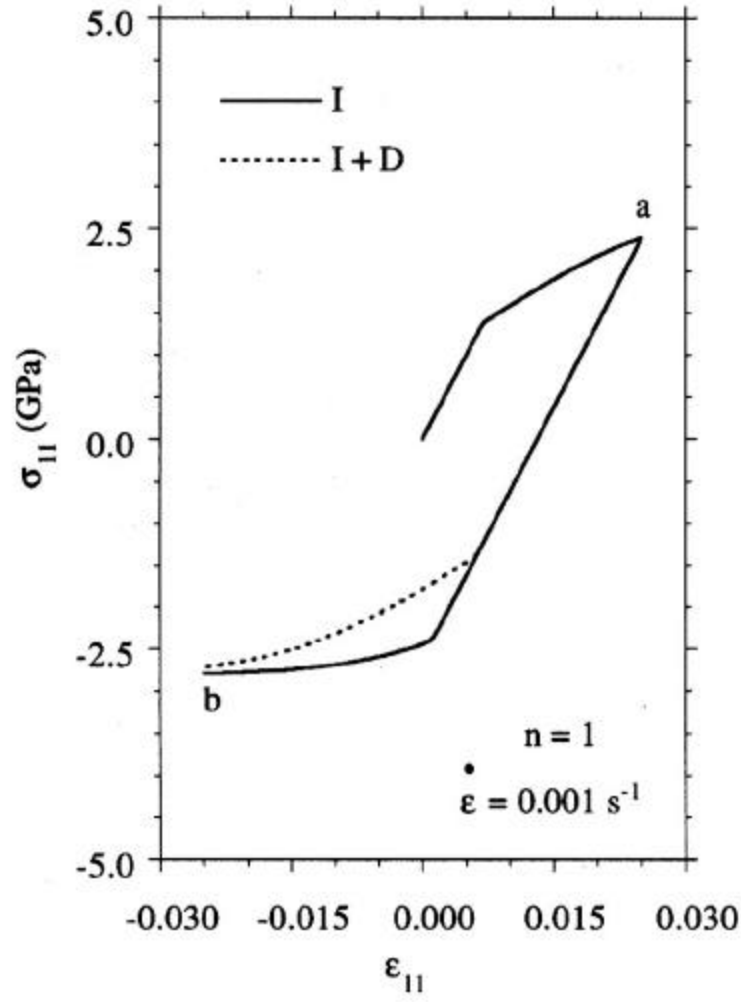


Fig. 11: Stress-strain curves upon loading, unloading and reversed loading for isotropic hardening (I) only, and with isotropic (I) and directional hardening (D), for $n = 1$ and associated constants with $m_2 = m_1$, $\dot{\epsilon} = 10^{-3} \text{ sec}^{-1}$.

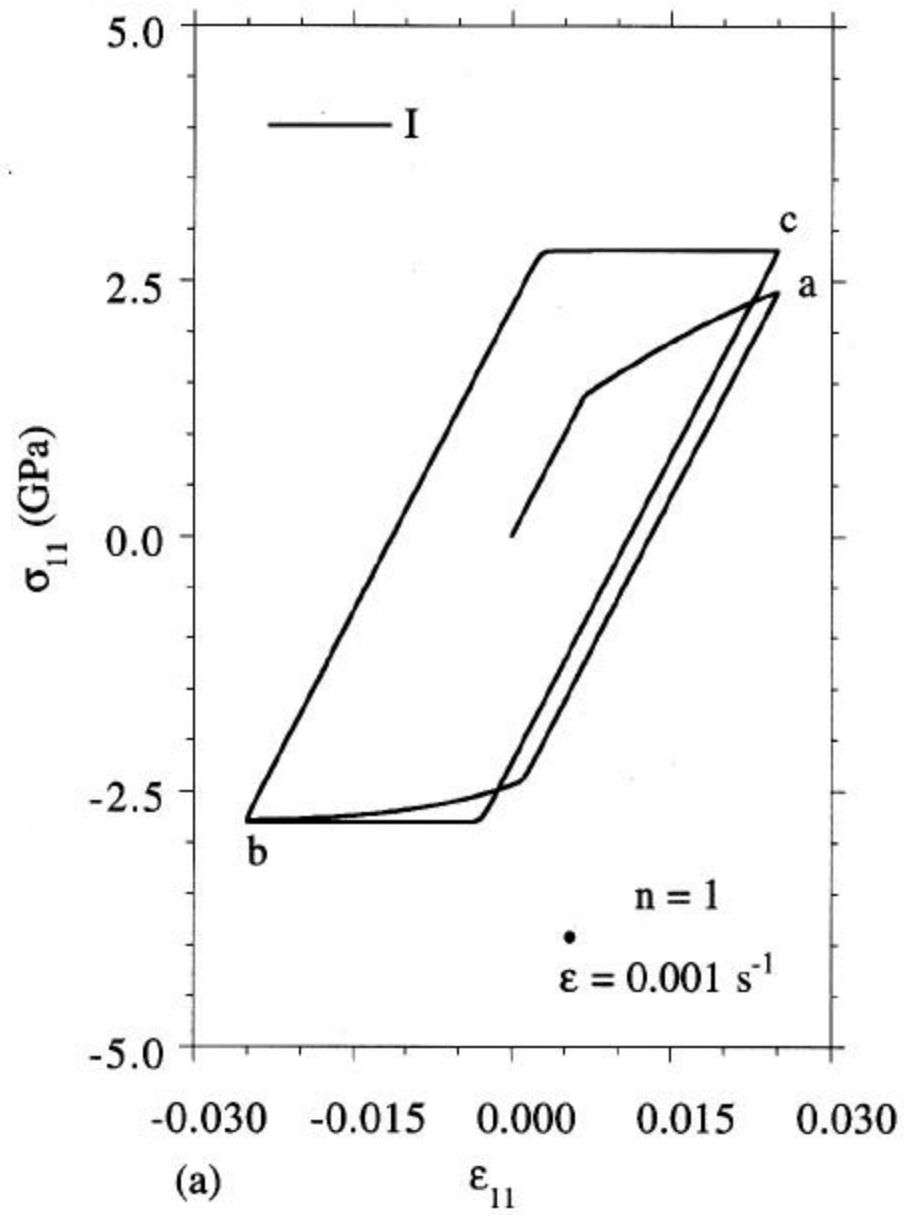


Fig. 12a: Cyclic stress-curves, $n = 1$ and associated constants, $m_2 = m_1$, $\dot{\epsilon} = 10^{-3} \text{ sec}^{-1}$, isotropic hardening only.

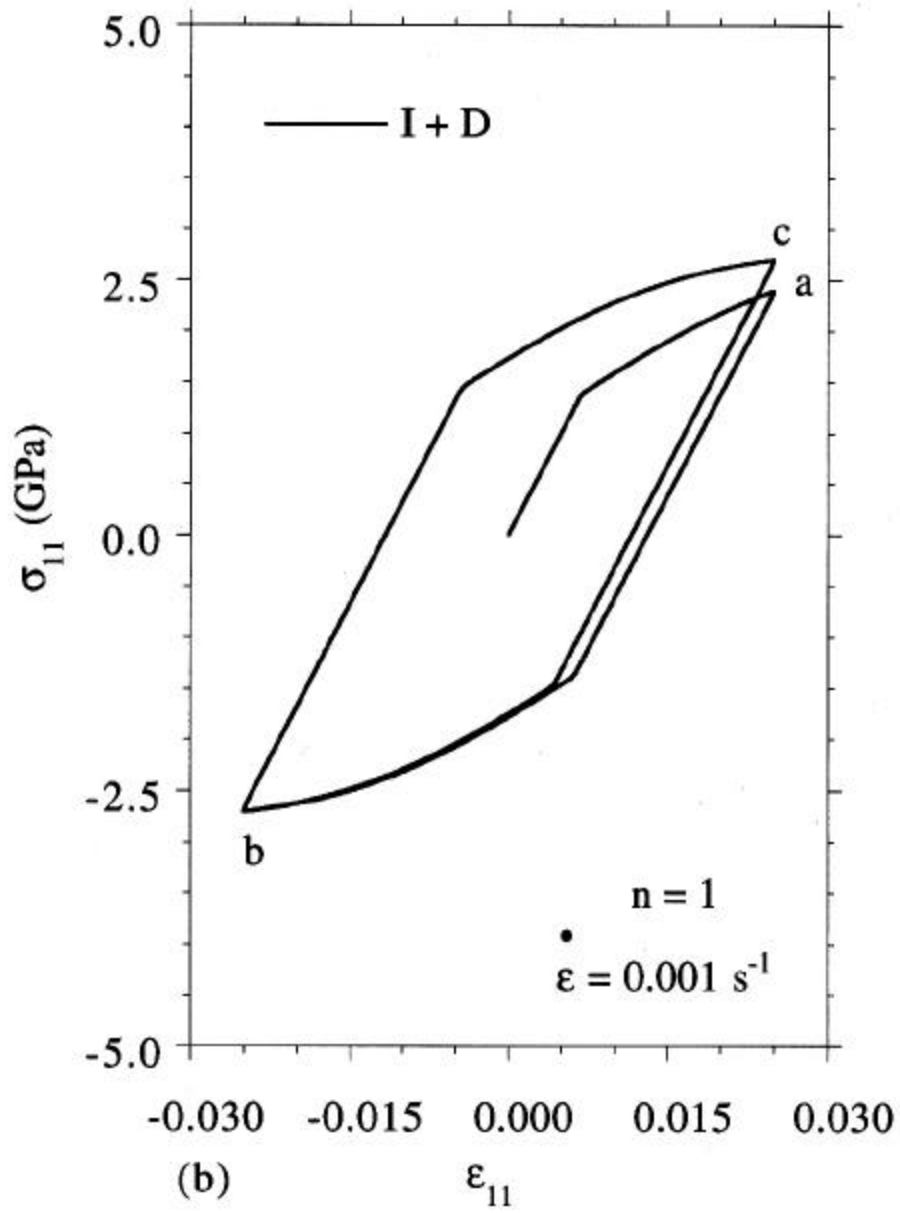


Fig. 12b: Cyclic stress-curves, $n = 1$ and associated constants,
 $m_2 = m_1$, $\dot{\epsilon} = 10^{-3} \text{ sec}^{-1}$, combined isotropic and directional hardening.

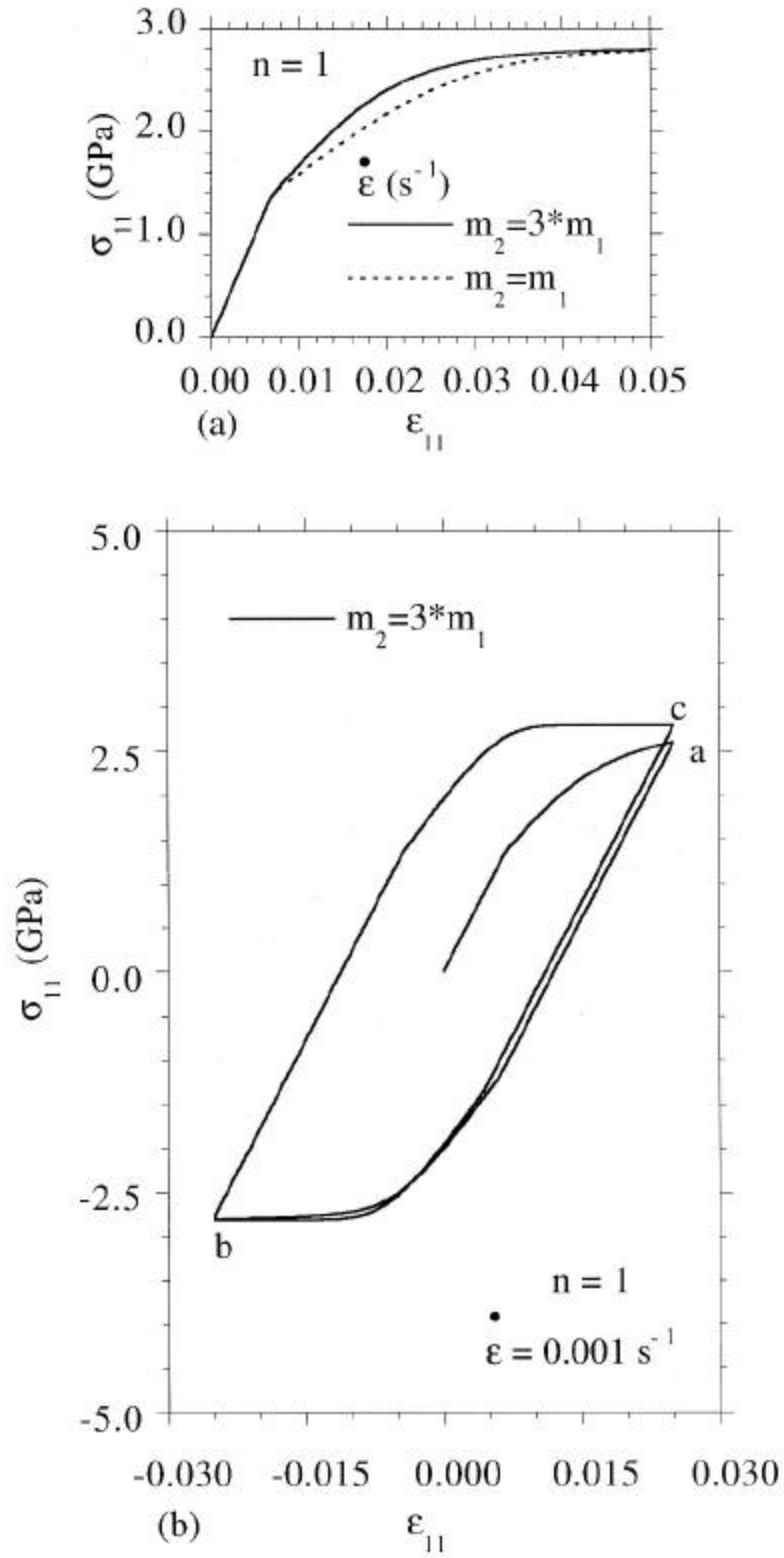


Fig. 13: Stress-strain curves for $n = 1$ and associated constants, $\dot{\epsilon} = 10^3 \text{ sec}^{-1}$,
 (a) monotonic straining $m_2 = m_1$ and $m_2 = 3m_1$,
 (b) cyclic straining with isotropic and directional hardening, $m_2 = 3 m_1$.

$$\eta = \frac{d\sigma}{dW_p} = \frac{1}{\sigma_{11}} \frac{d\sigma_{11}}{d\varepsilon_{11}^p}$$

B1900 + Hf

871°C

$\dot{\varepsilon}_{11} = 8.5 \times 10^{-6} \text{ sec}^{-1}$

$m_1 K_1 (Z_1 - Z_0) +$

$m_2 K_1 (Z_0 + Z_3)$

$m_1 K_1 (Z_1 + Z_3)$

Stress,
MPa

$K_1 (Z_1 + Z_3)$

Fig. 14: The isotropic and directional hardening components of B1900+Hf in an η - σ plot [from Chan et al. (1988)].

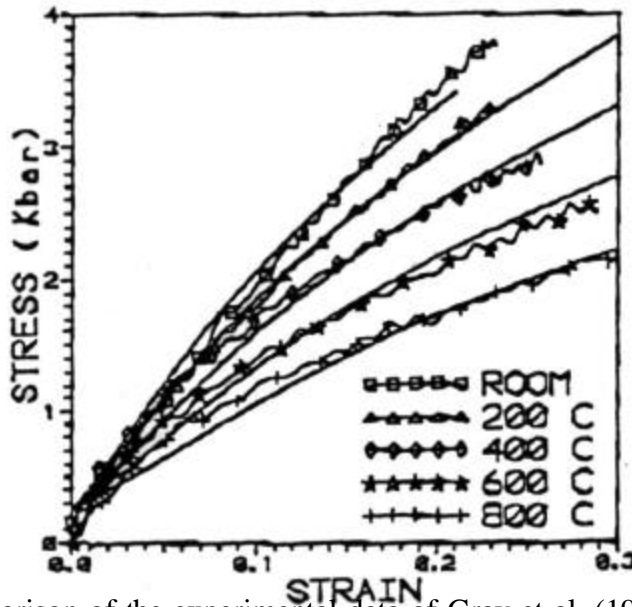


Fig. 15: Comparison of the experimental data of Gray et al. (1994) for compression with the Bodner-Partom model simulations taking $Z_1 \rightarrow Z_1(T)$, [from Bodner and Rajendran (1996)].

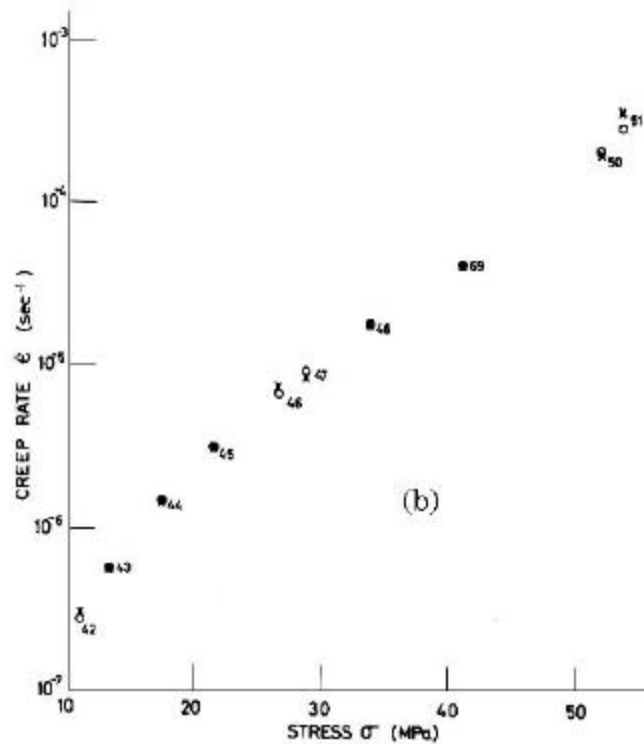
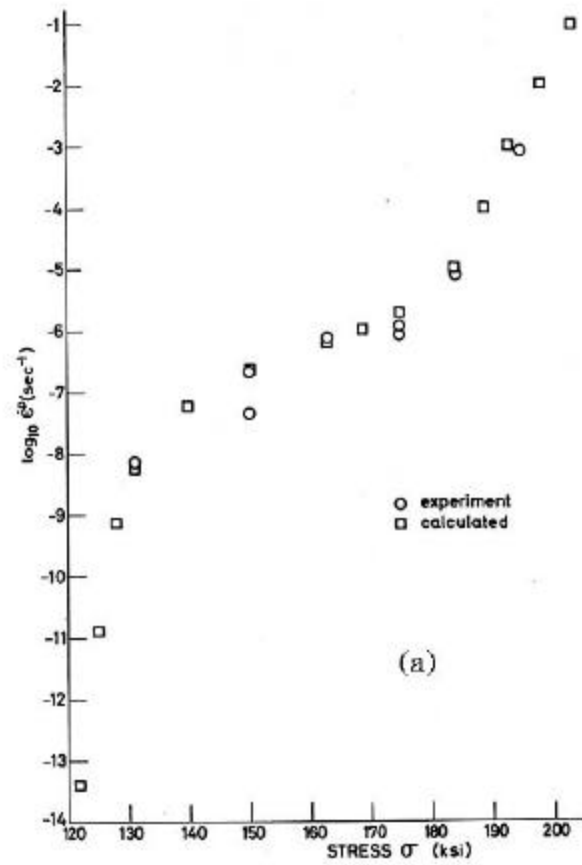


Fig. 16: Plots of stresses and associated steady strain rates.
 (a) René 95 at 1200°F (649°C), (100 ksi = 689.5 Mpa) [Bodner (1979)].
 (b) Copper at 550°C, o calculated, × test [Merzer (1982)].